Journal of Nuclear Materials 403 (2010) 167–183

Contents lists available at ScienceDirect

Journal of Nuclear Materials

journal homepage: www.elsevier.com/locate/jnucmat

The influence of iron on water radiolysis in cement-based materials

P. Bouniol

CEA, DEN, DPC, SCCME, Laboratoire d'Etude du Comportement des Bétons et des Argiles, F-91991 Gif-Sur-Yvette, France

ARTICLE INFO

Article history:
Received 24 July 2009
Accepted 15 June 2010

ABSTRACT

For the time being, assessing the H_2 source term generated by γ irradiated cement-based materials consists of simulating the radiolysis of the pore liquid on the only elementary reactions relating to the decomposition of alkaline water. Such incomplete description does not take into account the impurities contained in the cement and leads to underestimate the production of H_2. Systematically present in cement materials, iron is likely to influence radiolysis by the disturbance induced on radical chemistry throughout the irradiation period. The faster reactivity of e^-_{aq} and $OH^\cdot$ radicals on Fe(III) and Fe(II), respectively, than on H_2O_2 and H_2 is responsible for the lower recycling capability of the "Allen's chain reaction", allowing for H_2 to be preserved in a closed system. A critical review of reaction data about iron complexes (hydroxo-, peroxo-) is presented in order to build up an "iron" database. Radiolysis simulations in cement porewater in the presence of $Fe(OH)_3$ (considered as a model phase) show, as expected, an increase in the effective production of radiolytic H_2 and the co-existence of exotic valence Fe(IV) with Fe(II) and (III) during the irradiation period (γ).

© 2010 Elsevier B.V. All rights reserved.

1. Introduction

The production of gaseous H_2 by cement-based materials exposed directly or indirectly to ionising radiation results from the radiolysis of the residual water occupying part of the porosity of such materials. More specifically, it should be worded as the radiolysis of the H_2O solvent within an alkaline solution with a pH being often quite higher than 13, in equilibrium with the hydrated minerals of the concrete and more particularly with $Ca(OH)_2$ (portlandite). In the framework of that simplified chemical description, the review of the radiolytic mechanisms highlights an Allen-type reaction chain, similar to the known one at neutral pH [1], but characterised by faster kinetics [2]. Hence, at a high pH, the "classic" chain reaction

$$OH^\cdot + H_2 \rightarrow H^\cdot + H_2O \quad k = 4.2 \times 10^7\ M^{-1}\ s^{-1} \tag{1}$$

$$H^\cdot + H_2O_2 \rightarrow OH^\cdot + H_2O \quad k = 3.6 \times 10^7\ M^{-1}\ s^{-1} \tag{2}$$

becomes:

$$O^{\cdot -} + H_2 \rightarrow e^-_{aq} \quad k = 1.2 \times 10^8\ M^{-1}\ s^{-1} \tag{3}$$

$$e^-_{aq} + HO_2^- \rightarrow O^{\cdot -} + OH^- + H_2O \quad k = 3.5 \times 10^9\ M^{-1}\ s^{-1} \tag{4}$$

The predictable consequence of a faster rate in the new reaction chain is a better efficiency in the destruction of H_2 in an alkaline environment, which constitutes an interesting result from an operational standpoint (e.g., reduction in the quantity of gases emitted within disposal sites for cemented radioactive-wastes). Nevertheless, in order to describe the radiolytic process in irradiated cement matrices (very complex chemical environment including many impurities like transition elements and organics), the simulations carried out with the simplified chemical system may underestimate the production of H_2 due to an excessive recycling rate. That is translated into a gradual discrepancy between experiment and simulation in the case of a cement matrix irradiated (γ) within a closed system for a long time. According to the hypothesis in which the primary yields values used for simulation purposes are realistic in cement porewater, the lack in the calculated production of H_2 results in fact from an incomplete description of the secondary reactions system. The missing reactions include those concerning especially the species capable of quenching e^-_{aq} and $O^{\cdot -}$ and inducing consequently a less effective alkaline Allen's chain. In that regard, the species associated with transient elements are ideal candidates for participating in such mechanism by involving simultaneously several oxidation levels. The most common example includes the species of Fe(II) and Fe(III), which are likely to mobilise radicals with a potentially faster reaction chain than the Allen's chain (generic writing with convention $e^-_{aq} = H_2O^-$):

$$O^{\cdot -} + Fe(II) \rightarrow O^{2-} + Fe(III) \quad k \approx 10^8\text{–}10^9\ M^{-1}\ s^{-1} \tag{5}$$

$$e^-_{aq} + Fe(III) \rightarrow H_2O + Fe(II) \quad k \approx 10^{10}\ M^{-1}\ s^{-1} \tag{6}$$

Under those conditions, the survival rate of H_2 in solution may be higher since the attack of radical $O^{\cdot -}$ aims preferentially at Fe(II) and not at H_2. Such a mechanism seems probable in a cement environment where iron is present under several forms. In addition, Bibler [3,4] has suggested that adding αFe_2O_3 (hematite) to neat cement increases the partial pressure of H_2 by a factor exceeding

E-mail address: pascal.bouniol@cea.fr

0022-3115/$ - see front matter © 2010 Elsevier B.V. All rights reserved.
doi:10.1016/j.jnucmat.2010.06.020

3 for a γ dose rate of 1.4×10^5 Gy/h at 45 °C. However, a careful perusal of publications reveals that the tests were conducted with different cement types (Portland cement and high alumina cement) and different water proportions (water/cement ratio of 1.4 and 0.69). Consequently, the demonstration is not very conclusive and would need to be repeated under stricter operating conditions.

In the perspective of increasing the understanding of the influence of iron on the radiolysis of water within cement matrices, it would seem timely to establish in advance a summary of the available knowledge on the chemistry of iron in alkaline media and in the presence of radical species, if only to have at hand a minimum chemical model allowing for a better interpretation of the results. In the case where the significant role of iron would be confirmed in the radiolysis, that model could be integrated systematically with the current model based on the overall secondary reactions inventoried in the water with an alkaline pH [2]. Studying the chemistry of iron in the context of the radiolysis is also interesting, since it consolidates the required knowledge base for addressing corrosion under irradiation, a close theme to the many operational issues in the field of nuclear industry (corrosion of rebars, lining steels, etc.). After a presentation of the status of iron within the cement materials, this paper gives a preliminary review of the iron chemistry under radiation from literature data. As an implementation, water radiolysis model in the presence of iron is tested with two simulation examples. The possible contribution of the porous medium through the high specific area or the confinement effect in the finest pore sizes [5,6] is considered as negligible in these simulations.

2. Iron in neat cement paste

2.1. Origin of iron in cement materials

There are multiple iron sources in cement materials with both intrinsic and environmental origins (Table 1). The systematic presence of iron in the rock used for manufacturing concrete leads first of all to the formation of calcium aluminoferrite (also called C_4AF for $4CaO{\cdot}(Al, Fe)_2O_3$) in a proportion ranging from 5% to 15% of Portland cement. Later on, the hydration of that component generates ferric iron, which partakes in the formation of various materials where the element is present in solid solution (calcium monosulphoaluminate and monocarboaluminate and, to a lesser degree, hydrogarnet and ettringite). The iron concentration remains generally insufficient for iron oxides, oxihydroxides or hydroxides to crystallise directly. However, such components may be present as aggregates in concretes for radiation-protection purposes due to their γ-radiation mitigation property [7]. In that case, they constitute a significant source of iron in the form of hematite Fe_2O_3 (very stable, the most frequent use), goethite FeO(OH) or limonite $FeO(OH){\cdot}nH_2O$ (badly defined compound, metastable).

Except in the specific case of an intentional addition, iron is also present under a metallic form. As a matter of fact, by simple wear, the grinding process with expendable steel balls (consumables) generates particles with their surface probably covered with Fe(II and III) mixed oxidation products as early as the mixture with water. The same thing applies to the steel bars used for concrete armatures, which are often covered with yellow-orange rust. At that point, the interface with the cement neat constitutes an additional source of Fe(III), although localised, with the presence of ferrihydrite $Fe(OH)_3$. Lastly, a special mention should be made about the frequent addition of soluble Fe(II) sulphate at the end of the concrete-manufacturing process. The purpose of that operation is to reduce the traces of Cr(VI) in the cement into Cr(III), which is not toxic to cement-plant workers.

Table 1
Origin of iron in cement-based materials.

Systematic endogenous iron	Optional exogenous iron
C_4AF (minor component of cement)	Dense aggregates (radiation shielding concrete)
Fine steel particles (grinding process)	Steel armatures (reinforced concrete)
	Fe(II) sulphate (reducing additive in cement)

2.2. Iron concentration in the pore liquid

2.2.1. Host minerals

The chemical variability of components, the diversity of cement materials and the multiplicity of the potential host phases of iron make it possible to contemplate a rather wide spectrum of concentrations at equilibrium within the pore liquid. In fact, the total iron concentrations measured in various neat Portland cements vary over at least two orders of magnitude (10^{-7}–10^{-5} M) without being able to find a representative median value. In that field, it must also be recognised, however, that close to detection limits, all experimental data below 10^{-6} M are rather uneven in quality. Overall, concentrations tend to decrease when the water/cement relationship and the age of the material both increase. Among the identified host minerals, the monosulphated or monocarbonated aluminoferritic phases (known under the "AFm" acronym) generated by the hydration of the cement seem to be the best candidates, by reference to the solubility of iron-bearing poles and to their thermodynamic stability [8]:

$$Ca_4Fe_2SO_4(OH)_{12}\cdot 6H_2O \rightarrow 4Ca^{2+} + 2Fe(OH)_4^- + SO_4^{2-} + 4OH^- + 6H_2O \quad (K_s = 10^{-33.2})$$

$$Ca_4Fe_2CO_3(OH)_{12}\cdot 5H_2O \rightarrow 4Ca^{2+} + 2Fe(OH)_4^- + CO_3^{2-} + 4OH^- + 5H_2O \quad (K_s = 10^{-35.5})$$

In fact, those phases are more stable than their trisulphated counterparts (known under the "AFt" acronym), especially the Fe-ettringite, and display the particularity that their redissolution in alkaline media decreases as the pH increases (term in $[OH^-]^4$ in the solubility product), a phenomenon that is observed experimentally during hydration. Hence, the analysis of a pore liquid contained in Portland cement and with a water/cement weight ratio equal to 0.4 shows iron concentrations of 5×10^{-7} M for a pH of 13.1 after 1 day and 2×10^{-7} M for a pH of 13.3 after 150 days, respectively [9]. In the presence of abundant iron, on the contrary, the formation of specific phases of iron ($Fe(OH)_3$, Fe_2O_3, etc.) induces an increase in the solubility with the pH due to their amphoteric character (see Section 2.2.2).

Under normal manufacturing and operating conditions for cement materials (air contact, absence of irradiation), the solubilised iron in the pore liquid consists of ferric iron. If $FeSO_4$ is added, it is possible to consider that the same phenomenon applies, since the oxidation of ferrous iron is fast enough as early as the mixture phase. After oxidation, the solubility of Fe(III) exceeds 10^{-5} M, which leads to presume that, in such configuration and in the context of a very basic pH, the mineral in equilibrium forms a "high" solubility phase, consisting probably of $Fe(OH)_3$. It should be noted that, except in that case, a certain number of authors associated with Pr. F.P. Glasser assume that Fe(III) may precipitate in the form of $Fe(OH)_3$ (ferrihydrite or amorphous variety). In addition, they consider the latter to be a model phase for providing a good estimate of the iron in solution, at least at early age [8]. For long-term estimations, that phase is expected to be replaced by thermodynamically stable and less soluble goethite or hematite.

2.2.2. Speciation and concentration of Fe(III) at 25 °C

The complexation equilibria of the basic species of Fe(III) are well documented [10]. The selected data display the predominance field of five monomer complexes in relation to pH (Fig. 1a). It clearly shows that, within a cement medium characterised by a higher pH than 13, iron in solution is almost exclusively represented by the $Fe(OH)_4^-$ complex.

In the framework of a precise description of mineral equilibria, the above-mentioned AFm phases remain difficult to take into consideration for the time being due to the uncertainties relating to the substitution rate of iron and to the currently estimated values for solubility products. Since it is impossible to refer to a single mineral source, it seems wise to examine the solubility of Fe(III) within a field that is set on the basis of respective equilibria with $Fe(OH)_3$ (the most soluble) and Fe_2O_3 (the least soluble) and covers largely the interval between 10^{-7} and 10^{-5} M. The thermodynamic data selected for the mineralogical and complexation equilibria relating to the basic species of Fe(III) are displayed in Table 2. They help in the calculation of the total concentration of iron in solution and in the speciation in relation to the pH of the cement medium.

When considering a cement medium at 25 °C that contains at least portlandite in equilibrium (pH = 12.45), the pH is increased by adding NaOH up to approximately 0.45 mol/kg (pH = 13.47), a value beyond which the Debye–Hückel model with Davies extension becomes difficult to apply. The results of the composition calculations of the solution are shown in Fig. 2. In the field of the pH involved, it may be observed that:

- the total iron concentration increases according to a $\log_{10}[\Sigma Fe] = a\ pH + b$ relationship for $Fe(OH)_3$ and Fe_2O_3 (Fig. 2), whereas the calcium concentration decreases;
- on average, the total iron concentration in equilibrium with $Fe(OH)_3$ is about 8000 times higher than that associated with Fe_2O_3; and
- for a reference concentration of [Na] = 0.24 mol/kg (pH = 13.22), the concentration level of 7.42×10^{-4} M in equilibrium with $Fe(OH)_3$ appears sufficient to influence the water radiolysis, contrary to that corresponding to Fe_2O_3.

Based on the elements shown in Table 2, the calculated solubility values for $Fe(OH)_3$ seem relatively high and may even reach 10^{-3} M. They are generally higher than those obtained from other databases due to discrepancies in:

- solubility constants (to a minor extent);
- complexation constants (heavy impact on both speciation and solubility); and
- the calculation mode (lower solubility with zero ionic strength).

Since the solubility of $Fe(OH)_3$ may be multiplied by a factor of 10 when the pH increases by 1 unit, very variable iron concentrations must be expected in the pore solutions of cement pastes in relation to the alkaline concentrations (Na and K) of the latter. In fact, the high disparity observed in the experimental data concerning iron seems to depend upon the variability in the pH, irrespective of the nature of the solid phase in equilibrium. It should be noted that, with an alkaline concentration of 0.24 mol/kg, the pore liquid selected as reference lies rather in the average for Portland cements. The detailed composition of such a liquid, saturated with $Ca(OH)_2$ and $Fe(OH)_3$ at 25 °C and in contact with air, is shown in Table 3. Besides the $Fe(OH)_4^-$ complex representing more than 99.99% of the total iron and being responsible for the rather high solubility level of $Fe(OH)_3$, most other iron species appear to be completely negligible, particularly the dimer $Fe_2(OH)_2^{4+}$ complex. It is interesting to note that, in the case of the equilibrium with $Fe(OH)_3$, the concentration in a neutral complex is independent from the pH and constitutes a bottom value for total iron: $[Fe(OH)_3^\circ] = K_1K_2K_3\ K_{fer} = 2.165 \times 10^{-9}$ M, constant at 25 °C.

2.2.3. Influence of temperature on the solubility of $Fe(OH)_3$

The evolution of the system in equilibrium with $Fe(OH)_3$ in relation to temperature may be described through the thermodynamic data shown in Table 2 on the basis of a Van't Hoff formalism. The latter considers that, within a reaction in equilibrium characterised by a constant K, the variation in specific heat (ΔC_p) of species in solution is independent from temperature, which means, in other words, resolving the following differential system:

$$\frac{\partial(\Delta H_R)}{\partial T} = \Delta C_P = constant \quad \text{i.e. } \Delta H_R = (T - T_0)\Delta C_P + \Delta H_R^0$$

$$\frac{\partial \mathrm{Log}K(T)}{\partial T} = \frac{\Delta H_R}{RT^2}$$

With $\mathrm{Log}K_0 = -\frac{\Delta G_R^0}{RT_0}$, the integration of the system leads to the following Van't Hoff equation where $T_0 = 298.15$ K:

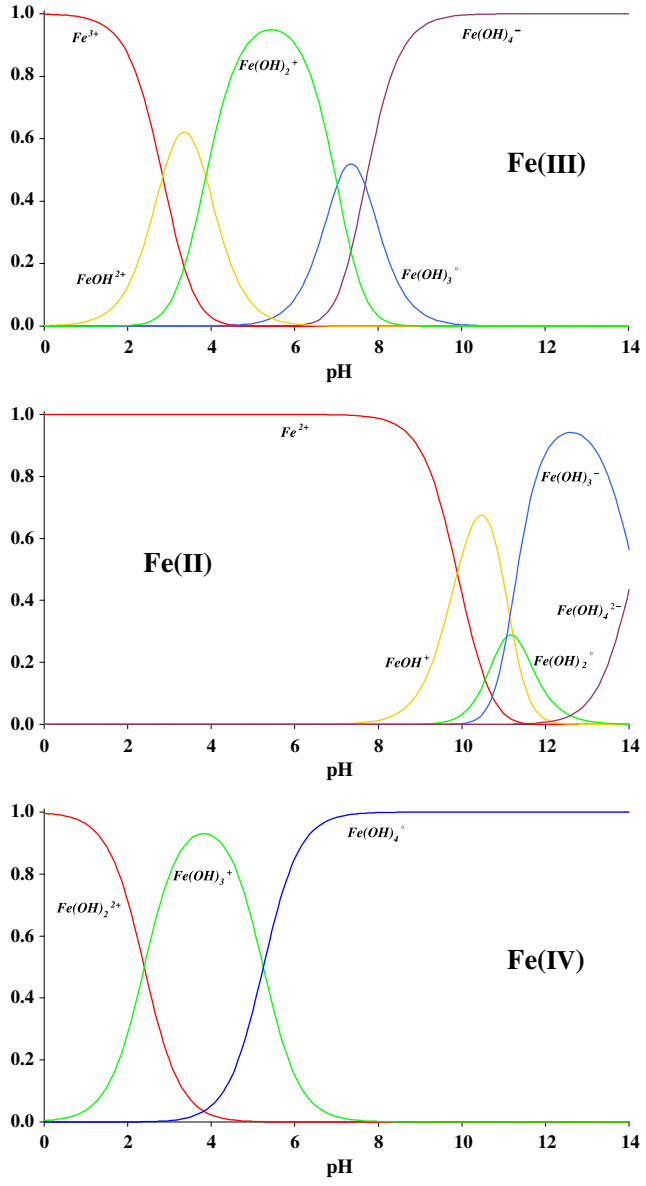

Fig. 1. Sillén diagram of Fe(III), (II) and (IV) established in relative proportion for a constant ionic strength (I = 0.226 mol/kg) representative of a cement pore liquid at 25 °C.

Table 2
Thermodynamic data on the mineralogical and complexation equilibria for Fe(III) used in the calculation of the pore solution at 25 °C.

Species	ΔG_f° (kJ/mol)	ΔH_f° (kJ/mol)	S° (J mol^{-1} K^{-1})	C_p° (J mol^{-1} K^{-1})	Equilibrium	Constant	$\log_{10} K$
Hematite αFe_2O_3	−744.249[b]	−826.23[b]	87.40[b]	103.85[b]	$\alpha Fe_2O_3 + 3H_2O \Longleftrightarrow 2Fe^{3+} + 6OH^-$	$K_{hem} = \frac{[Fe^{3+}]^2[OH^-]^6 \cdot \gamma_3^2 \gamma_1^6}{(H_2O)^3}$	−84.055[b]
Ferrihydrite $Fe(OH)_3$	−705.47[b]	−832.62[b]	104.6[b]	101.67[b]	$Fe(OH)_3 \Longleftrightarrow Fe^{3+} + 3OH^-$	$K_{fer} = [Fe^{3+}][OH^-]^3 \cdot \gamma_3 \gamma_1^3$	−38.11[b]
Water H_2O	−237.14[a,b]	−285.83[a,b]	69.95[a,b]	75.375[a,b]	$H_2O + H_2O \Longleftrightarrow H_3O^+ + OH^-$	$K_w = \frac{[H_3O^+][OH^-] \cdot \gamma_1^2}{(H_2O)^2}$	−13.995[a,b]
OH^-	−157.22[a,b]	−230.015[a,b]	−10.90[a,b]	−137.19[a,b]	Basic species		
Fe^{3+}	−16.28[b]	−49.0[b]	−278.4[b]	−77.8[b]	Basic species		
Complex 1 $Fe^{III}OH^{2+}$	−240.92[b]	−291.33[b]	−104.5[b]	−106.3[b]	$Fe^{3+} + OH^- \Longleftrightarrow FeOH^{2+}$	$K_1 = \frac{[FeOH^{2+}] \cdot \gamma_2}{[Fe^{3+}][OH^-] \cdot \gamma_3 \gamma_1}$	11.812[b]
Complex 2 $Fe^{III}(OH)_2^+$	−458.191[b]	−549.114[b]	−7.1[b]	−125.9[b]	$FeOH^{2+} + OH^- \Longleftrightarrow Fe(OH)_2^+$	$K_2 = \frac{[Fe(OH)_2^+]}{[FeOH^{2+}][OH^-] \cdot \gamma_2}$	10.521[b]
Complex 3 $Fe^{III}(OH)_3^\circ$	−656.017[b]	−802.726[b]	39.05[b]	−236.8[b]	$Fe(OH)_2^+ + OH^- \leftrightarrow Fe(OH)_3^\circ$	$K_3 = \frac{[Fe(OH)_3^\circ]}{[Fe(OH)_2^+][OH^-] \cdot \gamma_1^2}$	7.114[b]
Complex 4 $Fe^{III}(OH)_4^-$	−841.536[b]	−1058.849[b]	35.50[b]	−84.9[b]	$Fe(OH)_3^\circ + OH^- \Longleftrightarrow Fe(OH)_4^-$	$K_4 = \frac{[Fe(OH)_4^-]}{[Fe(OH)_3^\circ][OH^-]}$	6.184[b]
Complex 5 $Fe_2^{III}(OH)_2^{4+}$	−490.288[c]	−612.04[c]			$FeOH^{2+} + FeOH^{2+} \Longleftrightarrow Fe_2(OH)_2^{4+}$	$K_5 = \frac{[Fe_2(OH)_2^{4+}] \cdot \gamma_4}{[FeOH^{2+}][FeOH^{2+}] \cdot \gamma_2^2}$	1.480[c]

[a] CODATA.
[b] Selected values by Chivot [10].
[c] Martell and Smith [57].

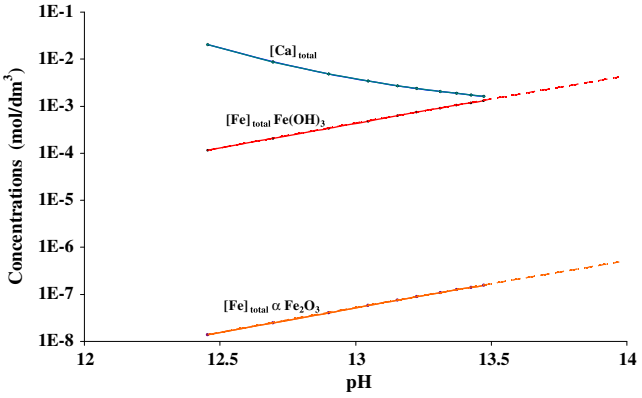

Fig. 2. Total iron and calcium concentrations in a 0.4 M NaOH solution saturated with $Ca(OH)_2$ and ferrihydrite or hematite in relation to pH at 25 °C.

$$\mathrm{Log}\,K(T) = -\frac{1}{R}\left(\frac{\Delta G_R^0}{T_0} + \left(T_0\Delta C_P - \Delta H_R^0\right)\left(\frac{1}{T_0} - \frac{1}{T}\right) + \Delta C_P\ \mathrm{Log}\frac{T_0}{T}\right)$$

That equation helps formulating the equilibrium constants in solution in the form of the following modified Arrhenius equation:

$$K(T) = A \cdot T^n \cdot e^{-E_a/RT}$$

For heterogeneous solid-solution equilibria, ΔC_P ceases to be independent from temperature and the integration of the system must take into account an expression of the ΔC_P of the solid phase in relation to that parameter. The expressions associated with the $Fe(OH)_3$ and Fe_2O_3 phases proposed by the NIST Database [11] are as follows:

$$C_{pFe(OH)_3} = 65.09091 + 182,2609 \times 10^{-3}T - 100.7172 \times 10^{-6}T^2 + 19.04084 \times 10^{-9}T^3 - 0.82534 \times 10^{6}T^{-2}$$

$$C_{pFe_2O_3} = 93.43834 + 108.3577 \times 10^{-3}T - 50.86447 \times 10^{-6}T^2 + 25.58683 \times 10^{-9}T^3 - 1.61133 \times 10^{6}T^{-2}.$$

After taking into account the data shown in Table 2, the constants of the different equilibria in relation to temperature (T in kelvins) are expressed following the modified Arrhenius equation and are gathered in Table 8. The solubility products of $Fe(OH)_3$ and Fe_2O_3 are respectively:

Table 3
Composition (molar) calculated at 25 °C of a simplified OPC pore solution resulting of equilibrium with portlandite and ferrihydrite.

Cations	Molecules	Anions
$[H_3O^+] = 8.03 \times 10^{-14}$	$[Ca(OH)_2^\circ] = 9.95 \times 10^{-4}$	$[OH^-] = 2.24 \times 10^{-1}$
$[Ca^{2+}] = 6.96 \times 10^{-4}$	$[NaOH^\circ] = 1.70 \times 10^{-2}$	$[Fe(OH)_4^-] = 7.42 \times 10^{-4}$
$[CaOH^+] = 6.87 \times 10^{-4}$	$[H_2O] = 55.39$	
$[Na^+] = 2.23 \times 10^{-1}$	$[H_2] = 3.82 \times 10^{-10}$	
$[Fe^{3+}] = 2.46 \times 10^{-35}$	$[O_2] = 2.60 \times 10^{-4}$	
$[FeOH^{2+}] = 5.98 \times 10^{-25}$	$[N_2] = 5.00 \times 10^{-4}$	
$[Fe(OH)_2^+] = 1.35 \times 10^{-15}$	$[Fe(OH)_3^\circ] = 2.16 \times 10^{-9}$	
$[Fe_2(OH)_2^{4+}] = 1.18 \times 10^{-46}$		

$$K_{fer}(T) = \exp\left(366.64 + \frac{9.86037 \times 10^6}{T^3} - \frac{49632.7}{T^2} - \frac{31127.3}{T} - 0.0255307T + 6.39796 \times 10^{-6}T^2 - 7.63361 \times 10^{-10}T^3 - 60.155\ \mathrm{Log}\,T\right)$$

$$K_{hem}(T) = \exp\left(-481.257 - \frac{1,18929 \times 10^8}{T^3} + \frac{598634}{T^2} - \frac{41268}{T} - 0.908173T + 7.13208 \times 10^{-4}T^2 - 2.98634 \times 10^{-7}T^3 + 112.182\ \mathrm{Log}\,T\right)$$

Discarding hematite because the concentrations at equilibrium are too low to influence the radiolysis, the variation of the solubility product of ferrihydrite in relation to temperature is our only concern. In spite of a variation of K_{fer} over four orders of magnitude between 0 and 100 °C, the solubility and speciation calculations with ferrihydrite in the context of a solution containing 0.24 mol/kg of NaOH and saturated with portlandite show a relatively slight variation in the total iron concentration within the same interval (Fig. 3). By comparison, the impact of temperature proves to be much more significant on the total calcium concentration.

2.3. Data on Fe(II) and Fe(IV) species

2.3.1. Speciation of Fe(II) and temperature evolution

The complexation equilibria relating to the basic species of Fe(II) are well documented [10] with a similar knowledge level

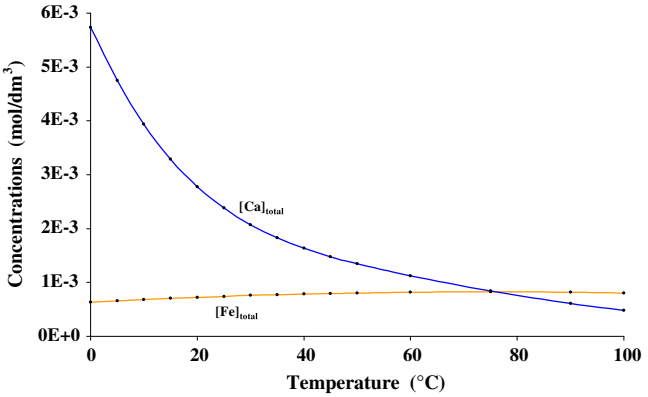

Fig. 3. Variation of total iron and calcium concentrations in NaOH solution at 0.24 mol/kg saturated with portlandite and ferrihydrite in relation to temperature.

as for Fe(III). The selected thermodynamic data (Table 4) display the predominance field of five monomer complexes in relation to pH at 25 °C (Fig. 1b). Within a cement medium characterised by a higher pH than 13, ferrous iron in solution is mostly represented by the $Fe(OH)_3^-$ complex, ranging approximately between 80% and 90%, with the $Fe(OH)_2^\circ$ and $Fe(OH)_4^{2-}$ complexes constituting the complement. Such relative "abundance" of species with an alkaline pH induces many reactions with the products of water radiolysis (see Section 3.2).

The evolution of the complexation constants of Fe(II) in relation to temperature is described through the thermodynamic data shown in Table 4 on the basis of a Van't Hoff formalism. Since the C_p value for the $Fe(OH)_4^{2-}$ complex is not available, it has been estimated on the basis of a *kriging* map in order to assess the evolution of the $K_{II/4}$ equilibrium with temperature. In the plan set in accordance with the number of ligands and of charges of the different complexes, the method consists in providing the missing data from the C_p variation gradients observed in all plan directions. The table of the C_p data for the complexes of Fe(II) and Fe(III), together with the resulting map, provide a C_p value of 30.7 J mol^{-1} K^{-1} for the $Fe(OH)_4^{2-}$ complex.

After taking into consideration the values shown in Table 4, the constants of the different equilibria in relation to temperature (T in kelvin) are expressed following the modified Arrhenius equation and are gathered in Table 8. The solubility product of $Fe(OH)_2$ is:

$$K_{hyd}(T) = \exp\left(246.215 + \frac{8.49754\times10^{6}}{T^3} - \frac{42772.8}{T^2} - \frac{15937.3}{T} - 0.0188886T + 5.33657\times10^{-6}T^2 - 6.91752\times10^{-10}T^3 - 39.0545\ \mathrm{Log}\,T\right)$$

established with [11]:

$$C_{phyd} = 56.70701 + 132.1357\times10^{-3}T - 83.59967\times10^{-6}T^2 + 17.25465\times10^{-9}T^3 - 0.711267\times10^{6}T^{-2}$$

According to the hypothesis where radiolysis may lead to significant concentrations of Fe(II), the integration of the solubility product of ferrous iron hydroxide must be contemplated due to potential precipitation. In the context of a model cement solution containing 0.24 mol/kg of NaOH and saturated with portlandite, the required concentration of total Fe(II) to reach equilibrium is 2.354×10^{-6} M at 25 °C. The evolution of the solubility product in relation to temperature is reflected by a very limited variation of concentrations at equilibrium in a field ranging from 0 to 100 °C, with values remaining slightly above to 2×10^{-6} M.

2.3.2. Speciation of Fe(IV)

Although it does not apply to standard thermodynamic conditions within cement media, the chemistry of Fe(IV) is systematically involved under irradiation with the occurrence of very reactive and highly-oxidising species (see Section 3). The level of knowledge concerning those unstable species is still very limited with only a constant value for the following complexation equilibrium:

$$Fe^{IV}(OH)_2^{2+} + OH^- \Longleftrightarrow Fe^{IV}(OH)_3^+ \quad pK_a = 2\ [12] \tag{7}$$

i.e.,

$$K_{IV/1} = \frac{[Fe(OH)_3^+]}{[Fe(OH)_2^{2+}][OH^-]\cdot\gamma_2} = \frac{K_a}{K_w} = 10^{11.9953}$$

Considering that there is at least one other complex (especially the $Fe^{IV}(OH)_4^\circ$ neutral complex) for higher pH values [13], the equilibrium constant of the $Fe^{IV}(OH)_4^\circ/Fe^{IV}(OH)_3^+$ couple is estimated by default on the basis of the mapping (kriging) of the known pK_a values for the different complex couples and oxidation levels II, III and IV. In the reference system set according to the equilibrium grade and oxidation level of the species, the collected data allocate a pK_a of 5.11 to the $Fe^{IV}(OH)_4^\circ/Fe^{IV}(OH)_3^+$ couple.

$$\text{Equilibrium } Fe^{IV}(OH)_3^+ + OH^- \Longleftrightarrow Fe^{IV}(OH)_4^\circ \tag{8}$$

is therefore characterised by the following constant:

$$K_{IV/2} = \frac{[Fe(OH)_4^\circ]}{[Fe(OH)_3^+][OH^-]\cdot\gamma_1^2} - \frac{K_a}{K_w} = 10^{8.8853}$$

On the basis of both equilibria under consideration, the predominance domain of the three monomer complexes of Fe(IV) in relation to pH at 25 °C is shown in Fig. 1c. In a cement medium characterised by a higher pH than 13, Fe(IV) in solution may be

Table 4
Thermodynamic data on the mineralogical and complexation equilibria for Fe(II) at 25 °C.

Species	ΔG_f° (kJ/mol)	ΔH_f° (kJ/mol)	S° (J mol^{-1} K^{-1})	C_p° (J mol^{-1} K^{-1})	Equilibrium	Constant	$\log_{10} K$
Iron hydroxide $Fe(OH)_2$	−491.96[a]	−574.04[a]	87.864[a]	81.13[d]	$Fe(OH)_2 \Longleftrightarrow Fe^{2+} + 2OH^-$	$K_{hyd2} = [Fe^{2+}][OH^-]^2\cdot\gamma_2\gamma_1^2$	−38.110[a]
Fe^{2+}	−90.53[a]	−90.0[a]	−101.6[a]	−33.0[a]	Basic species		
Complex 1 $Fe^{II}OH^+$	−273.44[a]	−320.60[a]	−28.3[a]	62.8[a]	$Fe^{2+} + OH^- \Longleftrightarrow FeOH^+$	$K_1 = \frac{[FeOH^+]}{[Fe^{2+}][OH^-]\cdot\gamma_2}$	4.501[a]
Complex 2 $Fe^{II}(OH)_2^\circ$	−447.23[a]	−542.00[a]	45.27[a]	75.3[a]	$FeOH^+ + OH^- \Longleftrightarrow Fe(OH)_2^\circ$	$K_2 = \frac{[Fe(OH)_2^\circ]}{[FeOH^+][OH^-]\cdot\gamma_1^2}$	2.903[a]
Complex 3 $Fe^{II}(OH)_3^-$	−620.44[a]	−809.42[a]	−37.5[a]	167.3[a]	$Fe(OH)_2^\circ + OH^- \Longleftrightarrow Fe(OH)_3^-$	$K_3 = \frac{[Fe(OH)_3^-]}{[Fe(OH)_2^\circ][OH^-]}$	2.801[a]
Complex 4 $Fe^{II}(OH)_4^{2-}$	−774.81[a]	−1072.86[a]	−170[a]	30.7[b]	$Fe(OH)_3^- + OH^- \Longleftrightarrow Fe(OH)_4^{2-}$	$K_4 = \frac{[Fe(OH)_4^{2-}]\cdot\gamma_2}{[Fe(OH)_3^-][OH^-]\cdot\gamma_1^2}$	−0.499[c]

[a] Selected values by Chivot [10].
[b] Extrapolated value by kriging method.
[c] NIST-JANAF [11].

practically assimilated with the neutral $Fe(OH)_4^\circ$ complex. No thermodynamic data being available, equilibria related to Fe(IV) cannot be described as a function of temperature.

3. Iron chemistry under radiation

3.1. Preliminary considerations

3.1.1. Occurrence of Fe(IV)

Since investigations on Fe(IV) are relatively recent, the implication of that exotic valence started only to be mentioned frequently in the 1990s. From a general standpoint, iron in solution only reaches oxidation level IV in the presence of the reactive species of oxygen (ROS), like ozone (a small amount of O_3 is produced by radiolysis) [14]:

$$Fe^{2+} + O_3 \rightarrow FeO^{2+} + O_2 \quad k = 8.3 \times 10^5\ M^{-1}\ s^{-1} \tag{9}$$

The species formed in very acid environments is ferryl ion (FeO^{2+}) to which the adjunction of a water molecule induces in principle the equivalent complex, $Fe(OH)_2^{2+}$. Although the latter would only exist as a transient state with a very low pH [15], it may be stabilised to a higher pH [12].

A second formation pathway for Fe(IV), and particularly for the ferryl ion, is associated with the action of hydrogen peroxide (a primary species of water radiolysis) on ferrous iron in the framework of an issue closely related to Fenton's reaction, as follows:

$$Fe^{2+} + H_2O_2 \rightarrow Fe^{3+} + OH^\cdot + OH^- \quad k = 5.2 \times 10^1\ M^{-1}\ s^{-1} \tag{10}$$

In fact, a considerable number of studies deal with that reaction and its variations, inasmuch as it is likely to provide very oxidising $OH^\cdot$ radicals, which are at the base of many processes to eliminate organic pollutants in soils or industrial effluents. In addition, many biological studies provide an equivalent contribution regarding the role of free radicals in the cellular metabolism. Nevertheless, by confirming experimentally the oxidising action of iron in an aqueous solution doped with hydrogen peroxide (or ozone), most authors are currently suggesting a series of reaction mechanisms discarding the Fenton-reaction interpretation validated by Haber and Weiss [16]. The new meaning of the reaction implies the formation of the ferryl ion, which would constitute the main oxidising species, as suggested before by a previous study [17], as follows:

$$Fe^{2+} + H_2O_2 \rightarrow Fe^{IV}O^{2+} + H_2O \quad k = 5.2 \times 10^1\ M^{-1}\ s^{-1} \tag{11}$$

As discussed further in Section 3.2.1, Reaction (11), however, cannot constitute a generic mechanism since it is not elementary and since its real products strongly depend on the pH. In this way, such a new description still allows the production of $OH^\cdot$ radicals but only for very low pH values (<1).

In very alkaline media, the attack of a hydroxyl complex of Fe(III) by oxidising radicals constitutes the third mode to obtain Fe(IV) species in solution [18], theoretically in the form of hydroxyl complexes. With due account of the significant value of the corresponding rate constant, the latter constitutes undeniably the main formation pathway of Fe(IV) under gamma irradiation in cement media, as follows:

$$Fe^{III}(OH)_4^- + OH^\cdot \rightarrow Fe^{IV}(OH)_4^\circ + OH^- \quad k = 8.5 \times 10^7\ M^{-1}\ s^{-1} \tag{12}$$

In brief, except for the rather marginal formation pathway with O_3, all conditions seem to be gathered to observe valence IV of iron within a cement medium under irradiation, which represents an environment characterised by a large variety of oxidising species, either radicalar ($O^{\cdot -}$, $O_2^{\cdot -}$) or not (O_2, HO_2^-). For information purposes, oxidation levels V (hypoferrate) and VI (ferrate), which are stable in alkaline media, also exist in other contexts, but do not seem to result from the oxidation mechanisms of Fe(III) induced by irradiation [18,19].

3.1.2. Occurrence of Fe(II)

Contrary to Fe(IV) the existence of which presents a relatively new character in the study of radiolysis in alkaline media, the occurrence of Fe(II) under the same conditions does not constitute an exceptional phenomenon. From a solution containing Fe(III) initially, it is in fact easy to obtain ferrous iron by reaction with the aqueous electron [20], as follows:

$$Fe^{3+} + e_{aq}^- \rightarrow Fe^{2+} + H_2O \quad k = 6.0 \times 10^{10}\ M^{-1}\ s^{-1} \tag{13}$$

The kinetic constant of that reaction is very high and even exceeds that of dioxygen reduction, the presence of which is frequent as a radiolytic by-product, as follows:

$$O_2 + e_{aq}^- \rightarrow O_2^{\cdot -} + H_2O \quad k = 1.9 \times 10^{10}\ M^{-1}\ s^{-1}\ [21] \tag{14}$$

The occurrence of ferrous iron under irradiation is the indispensable condition for initiating the chain reaction mentioned above, which is faster than the Allen chain, thus preserving H_2 against the attack of oxidising radicals, as follows:

$$e_{aq}^- + Fe(III) \rightarrow H_2O + Fe(II) \tag{6}$$

$$O^{\cdot -} + Fe(II) \rightarrow O^{2-} + Fe(III) \tag{5}$$

3.1.3. Fe(II) and dioxygen

The literature offers a large number of examples of radicalar reactions with iron species where radiolysis is not involved. Hence, such mechanisms intervene in the auto-oxidation process of ferrous iron in aerated aqueous solution. Outside the presence of other oxidants, Fe(II) is in fact rapidly oxidised by aqueous dioxygen. The higher the pH is, the faster is also the process, since the complexed forms of iron have a higher reactivity to O_2 [22]. The rate constants calculated at 25 °C with zero ionic strength [23] increase significantly with the complexation level, as follows:

$$O_2 + Fe^{2+} \rightarrow O_2^{\cdot -} + Fe^{3+} \quad k = 8.75 \times 10^{-2}\ M^{-1}\ s^{-1} \tag{15}$$

$$O_2 + Fe^{II}OH^+ \rightarrow O_2^{\cdot -} + Fe^{III}OH^{2+}\ k = 2.41 \times 10^1\ M^{-1}\ s^{-1} \tag{16}$$

$$O_2 + Fe^{II}(OH)_2^\circ \rightarrow O_2^{\cdot -} + Fe^{III}(OH)_2^+\ k = 8.16 \times 10^4\ M^{-1}\ s^{-1} \tag{17}$$

By extrapolation, the estimated value for the reaction with the complex located immediately above may even be very high:

$$O_2 + Fe^{II}(OH)_3^- \rightarrow O_2^{\cdot -} + H_2O + Fe^{III}(OH)_3^\circ k = 1.17 \times 10^9\ M^{-1}\ s^{-1} \tag{18}$$

It can be noticed that reaction rates given by Santana-Casiano et al. [23] differ from the values found by King [24]. The probable explanation is that, in both cases, an overall oxidation constant is experimentally determined but with a different kinetic model (assuming the reaction rates partition). Literature data show anyway a remarkable evolution of reaction rates with pH (many orders of magnitude), suggesting an inner-sphere pathway for electron transfer to explain the faster rates observed with the complexed species [25].

Reactions (15)–(18) give rise to the formation of the superoxide radical, the role of which is ambivalent, since it is both oxidising in the presence of Fe(II) and reducing in the presence of Fe(III). Since radical $O_2^{\cdot -}$ reacts with Fe(III) and generates again O_2 and Fe(II), the previous reactions represent therefore true redox equilibria. In addition, the oxidation of Fe(II) by $O_2^{\cdot -}$ induces the formation of peroxide, which in turn is involved within a complementary

oxidation process of Fe(II). Starting from any Fe(II) complex (e.g., $Fe^{II}OH^+$), the action of dioxygen may be summarised ultimately by the following simplified mechanism:

$$Fe^{II}OH^+ + O_2 \Longleftrightarrow Fe^{III}OH^{2+} + O_2^{\cdot-} \quad k = 2.4 \times 10^1 \text{ and } k_R = 1.5 \times 10^8\ M^{-1}\ s^{-1}\ [26] \tag{19}$$

$$Fe^{II}OH^+ + O_2^{\cdot-} \rightarrow Fe^{III}OH^{2+} + O_2^{2-} \quad k = 1.0 \times 10^7\ M^{-1}\ s^{-1}\ [26] \tag{20}$$

$$O_2^{2-} + H_2O \Longleftrightarrow HO_2^- + OH^- \quad pK_a = 16.5 \tag{21}$$

$$HO_2^- + H_2O \Longleftrightarrow H_2O_2 + OH^- \quad pK_a = 11.68 \tag{22}$$

$$Fe^{II}OH^+ + H_2O_2 \Longleftrightarrow Fe^{II}OH - H_2O_2^+ \quad k = 3.1 \times 10^6\ [27] \text{ and } k_R = 2.2 \times 10^4\ M^{-1}\ s^{-1}\ [28] \tag{23}$$

$$Fe^{II}OH - H_2O_2^+ \rightarrow Fe^{IV}(OH)_3^+ \quad k = 1.87 \times 10^{-1}\ M^{-1}\ s^{-1}\ [28] \tag{24}$$

$$Fe^{II}OH^+ + Fe^{IV}(OH)_3^+ \rightarrow 2Fe^{III}(OH)_2^+ \quad k = 1.4 \times 10^5\ \text{(estimate)} \tag{25}$$

$$2Fe^{III}OH^{2+} + 2OH^- \Longleftrightarrow 2Fe^{III}(OH)_2^+ \quad pK_a = 3.47 \tag{26}$$

$$\text{Balance}: \quad 4Fe^{II}OH^+ + O_2 + 2H_2O \rightarrow 4Fe^{III}(OH)_2^+ \tag{27}$$

In detail and from a more marginal standpoint, that mechanism may be completed by the occurrence of the OH· radical (the most oxidising) from the "Haber–Weiss" reaction and from the decomposition complex of Fe(IV), as follows:

$$O_2^{\cdot-} + H_2O_2 \rightarrow O_2 + OH^- + OH^\cdot \quad k = 1.3 \times 10^{-1}\ M^{-1}\ s^{-1}\ [29] \tag{28}$$

$$Fe^{IV}(OH)_3^+ \rightarrow Fe^{III}(OH)_2^+ + OH^\cdot \quad k = 2\ s^{-1}\ [30] \tag{29}$$

$$Fe^{II}OH^+ + OH^\cdot \rightarrow Fe^{III}(OH)_2^+ \quad k \geqslant 4.5 \times 10^8\ M^{-1}\ s^{-1} \quad \text{according to [31]} \tag{30}$$

It should be noted that if the "Haber–Weiss" reaction is disputed [32], its iron-catalysed variant has even fewer reasons to exist, since the Fenton's reaction itself is questioned. The principle of the conventional interpretation is as follows:

$$Fe(III) + O_2^{\cdot-} \rightarrow Fe(II) + O_2 \tag{31}$$

$$Fe(II) + H_2O_2 \rightarrow Fe(III) + OH^- + OH^\cdot \quad \text{(Fenton's reaction)} \tag{32}$$

$$\text{Balance}: \quad O_2^{\cdot-} + H_2O_2 \rightarrow O_2 + OH^- + OH^\cdot \quad \text{("Haber –Weiss " reaction)} \tag{28'}$$

Considering the overall self-oxidation process of Fe(II), the following conclusions emerge:

- in the hypothesis that the "Haber–Weiss" reaction, whether catalysed or not, did not exist, a small amount of radical OH· would be produced in any case due to the decomposition of the Fe(IV) complex;
- in the absence of irradiation, the mechanisms mentioned above involve most of the key products of water radiolysis ($O_2^{\cdot-}$, H_2O_2, $OH^\cdot$), except for reducing radicals H· and e^-_{aq}; and
- those mechanisms ensure the complete and irreversible oxidation of the initial inventory of ferrous iron in solution.

Under gamma irradiation, however, radiolysis generates constantly a noticeable amount of highly reducing radicals e^-_{aq} and H· (primary products), accompanied by lesser reducing radicals $O_2^{\cdot-}$ (secondary product). Starting with an initial presence of Fe(III), it is then possible to reach a dynamic-equilibrium state leading to the simultaneous presence of Fe(II) and (III). Since radiolysis also generates oxidising radicals OH· (primary product) in about the same proportion, radiolysis must lead ultimately to the coexistence of Fe(IV), Fe(III) and Fe(II) for as long as the gamma irradiation lasts. As shown in Fig. 4, this coexistence is also subjected to a symproportionation of Fe(II) and Fe(IV), like in Reaction (25). Primary yields of products at pH 7 and 13 are summarised for gamma radiolysis in Table 5 and show a radicals population which is in majority.

3.1.4. Basic species and nomenclature

A critical review is under way of the data found in the literature concerning the reactivity of iron species in the field of radicalar chemistry and in the more specific field of radiation chemistry. Upon completion, the resulting compilation should provide the most comprehensive and especially the most consistent reaction list possible accounting for the evolution of iron species in alkaline media and under irradiation. Starting with a necessarily simplified composition of the cement environment (absence of organic products, reactive anions, other transition elements than iron), the iron species taken into account are limited to "hydroxo" and "peroxo" complexes, which means about 20 species involved in about 60 reactions (see Section 3.2). All valences being taken into account, the iron species detected in that framework are essentially hexacoordinated monomers, including the transient complexes of Fe(II) with H_2O_2. The three other listed dimer species, including a mixed species of Fe(II–III), illustrate the systematic character of the inventory, but play practically no role in the description of the chemistry of iron in alkaline media. In order to ease readability, the species are written according to a conventional way, but the equivalence with actual entities is given in Table 6.

3.1.5. Disparity among basic data

At a higher pH than 13 and at oxidation states II–IV, iron appears to be largely complexed with $Fe^{II}(OH)_3^-$, $Fe^{III}(OH)_4^-$ and $Fe^{IV}(OH)_4^\circ$ as respective dominant species. Under those forms, iron is considered more reactive than in the absence of ligand, but there are also paradoxically less reaction and kinetic data than at lower pH levels, since the mechanisms described in that context constitute the essential part of the documentation. Since a large number of reactions are lacking theoretically in alkaline media, the identified mechanisms with a low pH result therefore in an unbalanced description of the system in cement environments to the extent that:

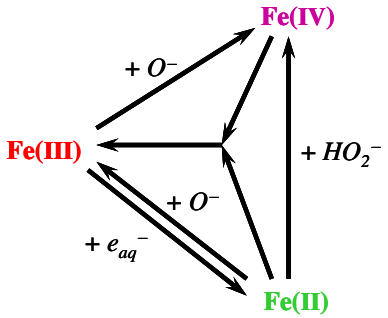

Fig. 4. Main relations between the three valences of iron present under gamma irradiation in alkaline medium.

Table 5
Set of primary yields for water radiolysis under β and γ radiation at 25 °C [33]; values (molecules/100 eV) must be multiplied by 1.036×10^{-7} to obtain G in moles per joule; radicalar products in bold characters.

pH	G_{H_2}	$G_{e^-_{aq}}$	G_H	G_{OH^-}	G_{-H_2O}[a]	$G_{H_3O^+}$	G_{OH}	$G_{H_2O_2}$	G_{HO_2}
7	0.45	**2.66**	**0.55**	0.10	9.63	2.76	**2.67**	0.72	**0**
13	0.425	**2.80**	**0.55**	0.50	10.80	3.30	**3.00**	0.60	**0**

[a] $G_{-H_2O} = G_{-water} + 2G_{H_3O^+} - G_{HO_2}$ due to the convention $e^-_{aq} = H_2O^-$.

Table 6
Nomenclature of the aqueous species of Fe(II, III, IV).

Oxidation level	Generic species	Effective entity	Conventional abbreviation
Fe(II)	Fe^{2+}	$Fe(H_2O)_6^{2+}$	Fe^{2+}
		$FeOH(H_2O)_5^{+}$	$FeOH^{+}$
	$FeO°$	$Fe(OH)_2(H_2O)_4^{\circ}$	$Fe(OH)_2^{\circ}$
	$HFeO_2^-$	$Fe(OH)_3(H_2O)_3^-$	$Fe(OH)_3^-$
	FeO_2^{2-}	$Fe(OH)_4(H_2O)_2^{2-}$	$Fe(OH)_4^{2-}$
	Transient	$FeH_2O_2(H_2O)_5^{2+}$	$FeH_2O_2^{2+}$
	Transient	$FeOH\ H_2O_2(H_2O)_4^{+}$	$FeOH\ H_2O_2^{+}$
	Transient	$Fe(OH)_2H_2O_2(H_2O)_3^{\circ}$	$Fe(OH)_2H_2O_2^{\circ}$
		$FeHO_2(H_2O)_5^{+}$	$FeHO_2^{+}$
	Fe_2O^{2+}	$Fe_2(OH)_2(H_2O)_8^{2+}$	$Fe_2(OH)_2^{2+}$
Fe(II) Fe(III)		$Fe_2HO_2(H_2O)_7^{4+}$	$Fe_2HO_2^{4+}$
Fe(III)	Fe^{3+}	$Fe(H_2O)_6^{3+}$	Fe^{3+}
		$FeOH(H_2O)_5^{2+}$	$FeOH^{2+}$
	FeO^{+}	$Fe(OH)_2(H_2O)_4^{+}$	$Fe(OH)_2^{+}$
	$HFeO_2^{\circ}$	$Fe(OH)_3(H_2O)_3^{\circ}$	$Fe(OH)_3^{\circ}$
	FeO_2^-	$Fe(OH)_4(H_2O)_2^-$	$Fe(OH)_4^-$
		$FeHO_2(H_2O)_5^{2+}$	$FeHO_2^{2+}$
	FeO_2^{+}	$FeOH\ HO_2(H_2O)_4^{+}$	$FeOH\ HO_2^{+}$
	Fe_2O^{4+}	$Fe_2(OH)_2(H_2O)_8^{4+}$	$Fe_2(OH)_2^{4+}$
Fe(IV)	FeO^{2+}	$FeO(H_2O)_5^{2+}$	$Fe(OH)_2^{2+}$
	$HFeO_2^{+}$	$FeO\ OH(H_2O)_4^{+}$	$Fe(OH)_3^{+}$
	FeO_2°	$FeO(OH)_2(H_2O)_3^{\circ}$	$Fe(OH)_4^{\circ}$

- they are not always representative of those prevailing at a high pH;
- whether representative or not, their impact is only very partly "propagated" at a high pH through acid–base and redox equilibria (Fig. 5).

3.2. Critical review of elementary processes[1]

3.2.1. Reactions of Fe(II) with H_2O_2

The behaviour of iron in irradiated cement media should not be examined without taking into account its many reactions with H_2O_2, a major and metastable radiolytic product. Abundant in the field of acid pH, the literature includes a large number of references to "Fenton's reaction", which is formulated generally with the Fe^{2+} ion as follows:

$$Fe^{2+} + H_2O_2 \rightarrow Fe^{3+} + OH^- + OH^{\cdot} \quad (10)$$

Such formulation, however, does not correspond to an actual mechanism and it is appropriate to replace it by a more elaborate reaction scheme for each complex of Fe(II). The variety of works on this topic is shown through the summary of Pignatello et al. [34] which gives an extended overview. The basic mechanism being selected for Fe^{2+} species is inspired by the Kremer's work [35] with respect to only Reactions (33), 33R and 34. It starts with the (reversible) formation of an intermediary complex (Reaction (33)). That complex is then rearranged into a hydroxyl form of the ferryl ion (Reaction (34)), the use of $Fe^{IV}(OH)_2^{2+}$ being preferred instead of FeO^{2+} because of writing consistency. The new complex decomposes slowly (Reaction (35)), without any reaction on itself [14]. Since the original constant $k_{35} = 1.3 \times 10^{-2}\ M^{-1}\ s^{-1}$ corresponds to kinetics of order 2 ($FeO^{2+} + H_2O$), the equivalent constant for order 1 is obtained by multiplying k_{35} by $[H_2O]$. In addition, the $FeIV(OH)_2^{2+}$ complex symproportionates with the Fe^{2+} ion according to two reaction pathways (Reactions (36a) and (36b)) [15,36,37]. It reacts also with H_2O_2 (Reaction (37)) and with HO_2 and OH radicals (Reactions (38) and (39)) [12,14,15,37].

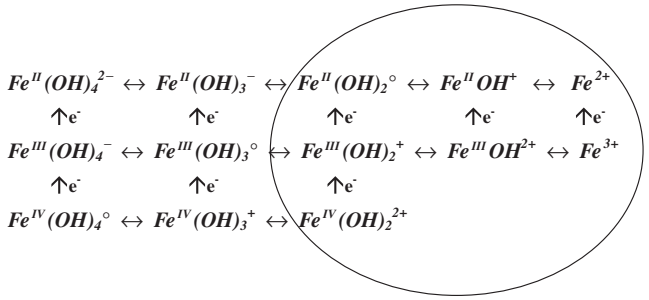

Fig. 5. Acid–base and redox relationships among the hydroxyl complexes of iron, with the circled domain corresponding to acidic species mostly studied in the literature.

$$Fe^{2+} + H_2O_2 \Longleftrightarrow Fe^{II} \cdot H_2O_2^{2+} \quad k = 52.4\ M^{-1}\ s^{-1}\ [35] \text{ and } k_R = 0.18\ s^{-1}\ [28] \quad (33)$$

$$Fe^{II} \cdot H_2O_2^{2+} \rightarrow Fe^{IV}(OH)_2^{2+} \quad k = 0.187\ s^{-1}\ [28] \quad (34)$$

$$Fe^{IV}(OH)_2^{2+} \rightarrow Fe^{III}OH^2 + +OH^{\cdot} \quad k = 7.2 \times 10^{-1}\ s^{-1}\ [14] \quad (35)$$

$$Fe^{2+} + Fe^{IV}(OH)_2^{2+} \rightarrow Fe^{3+} + Fe^{III}(OH)_2^{+}\ k = 7.7 \times 10^3\ M^{-1}\ s^{-1}\ [36] \quad (36a)$$

$$Fe^{2+} + Fe^{IV}(OH)_2^{2+} \rightarrow Fe_2^{III}(OH)_2^{4+} \quad k = 3.56 \times 10^4\ M^{-1}\ s^{-1}\ [36] \quad (36b)$$

$$H_2O_2 + Fe^{IV}(OH)_2^{2+} \rightarrow HO_2^{\cdot} + H_2O + Fe^{III}OH^{2+} \quad k = 9.5 \times 10^3\ M^{-1}\ s^{-1}\ [37] \quad (37)$$

$$HO_2^{\cdot} + Fe^{IV}(OH)_2^{2+} \rightarrow O_2 + H_2O + Fe^{III}OH^{2+}\ k = 2 \times 106\ M^{-1}\ s^{-1}\ [14] \quad (38)$$

$$OH^{\cdot} + Fe^{IV}(OH)_2^{2+} \rightarrow H_2O_2 + Fe^{III}OH^{2+}\ k = 1 \times 10^7\ M^{-1}\ s^{-1}\ [14] \quad (39)$$

The $Fe^{IV}(OH)_2^{2+}$ complex presents an indirectly or directly oxidising character according to the production of $OH^{\cdot}$ radicals or not (Reactions (35) and (36), respectively). Not supported by Kremer (as any radical else too), secondary production of $OH^{\cdot}$ radicals obviously remains the mechanism compatible with experimental results at very low pH. The best example is given by the well known behaviour of the Fricke dosimeter ($[Fe^{2+}] = 10^{-3}$ M, pH = 0.46 with H_2SO_4, air saturated) insofar as the global reaction is the oxidation of Fe^{2+} by H_2O_2 in the ratio 2:1. In order to explain such a result with a pseudo-first order kinetics (large excess of Fe^{2+} in comparison with H_2O_2), it is then necessary to add Reaction (40) which introduces a strong dependence towards pH:

$$H_3O^+ + Fe^{II} \cdot H_2O_2^{2+} \rightarrow 2H_2O + OH^{\cdot} + Fe^{3+} \quad k \approx 52\ M^{-1}\ s^{-1} \quad (40)$$

Simulations of the Fricke dosimeter made with Reactions (33)–(35), (36a), (36b), (37)–(40), complemented by reactions listed in sections ahead, indicate that k_{40} should have a value very close to the k_{33}'s one. At higher pH, Reaction (36), also reported in a recent work [38], constitutes the main oxidation path for Fe(II). The activation energies associated with Reactions 33, 35, 36a, 36b, 37 stand at 42 kJ/mol [39], 34, 42, 7 and 23 kJ/mol [37], respectively. Typical of the acid field, Reactions (33)–(35), (36a), (36b), (37)–(40) have practically no impact on the kinetics in alkaline media.

In the case of a pH between 9.5 and 11.1, Fe(II) is essentially represented by the $Fe^{II}OH^+$ complex, whereas Fe(IV) appears as $Fe^{IV}(OH)_3^+$, or even as the neutral $Fe^{IV}(OH)_4^{\circ}$ complex. In that field, the attack of the $Fe^{II}OH^+$ complex by H_2O_2 has also been studied

[1] Reactions are arbitrarily gathered into sections which do not constitute by themselves complete mechanisms.

and is similar to Mechanisms 33–36, but is also different by faster kinetics [30]. Reactions (45)–(47) are homologous to Reactions (37)–(39). Although undocumented, they have the same generic kinetic constants, as follows:

$$Fe^{II}OH^+ + H_2O_2 \Longleftrightarrow Fe^{II}OH \cdot H_2O_2^+ \quad k = 3.1 \times 10^6\ M^{-1}\ s^{-1}\ [27]$$
$$\text{and } k_R = 2.18 \times 10^4\ s^{-1}\ [28] \tag{41}$$
$$Fe^{II}OH \cdot H_2O_2^+ \rightarrow Fe^{IV}(OH)_3^+ \quad k = 0.187\ s^{-1}\ [28] \tag{42}$$
$$Fe^{IV}(OH)_3^+ \rightarrow Fe^{III}(OH)_2^+ + OH^\cdot \quad k = 2\ s^{-1}\ [30] \tag{43}$$
$$Fe^{II}OH^+ + Fe^{IV}(OH)_3^+ \rightarrow 2Fe^{III}(OH)_2^+ \quad k \geqslant 1.4 \times 10^5\ M^{-1}\ s^{-1} \tag{44}$$
$$H_2O_2 + Fe^{IV}(OH)_3^+ \rightarrow HO_2^\cdot + H_2O + Fe^{III}(OH)_2^+$$
$$k = 9.5 \times 10^3\ M^{-1}\ s^{-1}\ [37] \tag{45}$$
$$HO_2^\cdot + Fe^{IV}(OH)_3^+ \rightarrow O_2 + H_2O + Fe^{III}(OH)_2^+$$
$$k = 2 \times 10^6\ M^{-1}\ s^{-1}\ [14] \tag{46}$$
$$OH^\cdot + Fe^{IV}(OH)_3^+ \rightarrow H_2O_2 + Fe^{III}(OH)_2^+$$
$$k = 1 \times 10^7\ M^{-1}\ s^{-1}\ [14] \tag{47}$$

The calculated activation energy for Reaction (41) stands at 22.9 kJ/mol [27], since the values for Reactions (42)–(47) are unknown. The reverse rate, k_{-41}, is estimated from the following relationship: $k_m = (k_{-41} + k_{42})/k_{41}$, where k_m is equal to 0.007 M [28]. Symproportionation reaction 44 does not generate probably a dimer, and the value of k_{44} [14] constitutes theoretically a bottom limit.

In the rather limited predominance of the $Fe^{II}(OH)_2^\circ$ complex ($11.1 < pH < 11.2$), suitable data are not available excepted those concerning Reaction (48) with a rate constant of $k_{48} = 3.8 \times 10^9\ M^{-1}\ s^{-1}$ and an activation energy of 44.4 J/mol [27]. Calculated according to the previous method with k_{49} being equal to $0.187\ s^{-1}$, the reverse rate constant is therefore: $k_{-48} = 2.7 \times 10^7\ M^{-1}\ s^{-1}$. The rest of the mechanism may be copied on the previous scheme (Reactions (41)–(47)) by maintaining by default the rate constant values as bottom limits or as generic values (Reactions (52)–(54)), as follows:

$$Fe^{II}(OH)_2^\circ + H_2O_2 \Longleftrightarrow Fe^{II}(OH)_2.H_2O_2^\circ \tag{48}$$
$$Fe^{II}(OH)_2 \cdot H_2O_2^\circ \rightarrow Fe^{IV}(OH)_4^\circ \tag{49}$$
$$Fe^{IV}(OH)_4^\circ \rightarrow Fe^{III}(OH)_3^\circ + OH^\cdot \tag{50}$$
$$Fe^{II}(OH)_2^\circ + Fe^{IV}(OH)_4^\circ \rightarrow 2Fe^{III}(OH)_3^\circ \tag{51}$$
$$H_2O_2 + Fe^{IV}(OH)_4^\circ \rightarrow HO_2^\cdot + H_2O + Fe^{III}(OH)_3^\circ \tag{52}$$
$$HO_2^\circ + Fe^{IV}(OH)_4^\circ \rightarrow O_2 + H_2O + Fe^{III}(OH)_3^\circ \tag{53}$$
$$OH^\cdot + Fe^{IV}(OH)_4^\circ \rightarrow H_2O_2 + Fe^{III}(OH)_3^\circ \tag{54}$$

Starting from the modified Fenton's reaction (33), considered as slow, it is possible to observe that the value of the rate constant for derived Reactions (41) and (48) increases very significantly in relation to the complexation level. In the context of an even more alkaline medium, no information is currently available concerning potential reactions between higher complexes $Fe^{II}(OH)_3^-$ or $Fe^{II}(OH)_4^-$, and HO_2^-. Nevertheless, it would seem useful to refer to a symproportionation reaction with $Fe^{II}(OH)_3^-$ at least, in order to regulate the Fe(IV) concentration with a pH higher than 13. By default, it was allocated the same as Reaction (44), as follows:

$$Fe^{II}(OH)_3^- + Fe^{IV}(OH)_4^\circ \rightarrow Fe^{III}(OH)_3^\circ + Fe^{III}(OH)_4^- \quad k \geq 1.4 \times 10^5\ M^{-1}\ s^{-1} \tag{55}$$

3.2.2. Reactions of Fe(III) with H_2O_2 and HO_2^-

Ferric iron reacts poorly with hydrogen peroxide and generates the $Fe^{III}HO_2^{2+}$ complex, without any further possible evolution [26]. The rate constant of the reaction increases with the complexation of iron (Reactions (56) and (57)) and with the basic form of peroxide (Reaction (58)). In the latter case, however, the described reaction [40] involves species that do not share the same pH and caution is advised. The $Fe^{III}HO_2^{2+}$ complex decomposes according to Reaction (59), which is interpreted often by the equilibrium of Reactions (56)–(58) [30]. Its activation energy is equal to 8.8 kJ/mol [41]. The decomposition reaction $Fe^{III}HO_2^{2+} \rightarrow Fe^{2+} + HO_2^\cdot$, which is mentioned sometimes [42–44], and the related mechanism $Fe(III) + H_2O_2 \rightarrow Fe(II) + HO_2^\cdot + H^+$ (known as "Fenton-like reaction") seem unlikely and have been discarded. It should be noted that $Fe^{III}HO_2^{2+}$ and Fe^{2+} might be involved in the reversible formation of a mixed complex [26,41] (Equilibrium 60). The activation energy of Reaction (60) is 47.7 kJ/mol [41].

$$Fe^{3+} + H_2O_2 \rightarrow Fe^{III}HO_2^{2+} + H^+ \quad k = 4.48 \times 10^{-3}\ M^{-1}\ s^{-1}\ [30] \tag{56}$$
$$Fe^{III}OH^{2+} + H_2O_2 \rightarrow Fe^{III}HO_2^{2+} + H_2O$$
$$k = 2 \times 10^{-2}\ M^{-1}\ s^{-1}\ [42] \tag{57}$$
$$Fe^{3+} + HO_2^- \rightarrow Fe^{III}HO_2^{2+} \quad k = 9 \times 10^5\ M^{-1}\ s^{-1}\ [40] \tag{58}$$
$$Fe^{III}HO_2^{2+} \rightarrow Fe^{3+} + HO_2^- \quad k = 1.9 \times 10^3\ s^{-1}\ [41] \tag{59}$$
$$Fe^{III}HO_2^{2+} + Fe^{2+} \Longleftrightarrow Fe_2^{II,III}HO_2^{4+} \quad k = 6.8 \times 10^5\ M^{-1}\ s^{-1}$$
$$\text{and } k_R = 2.5 \times 10^4\ s^{-1}\ [41] \tag{60}$$

The impact of Reactions (56)–(60) seems very limited at a pH above 13 in the absence of data on potential reactions between more hydroxylated forms. The fairly stable $Fe^{III}HO_2^{2+}$ complex intervenes significantly in the result of the "Fenton reaction" [38], if only by monopolising a part of the peroxide.

3.2.3. Reactions of Fe(II) with $HO_2^\cdot$ and $O_2^{\cdot-}$

Ferrous iron is oxidised by the hydroperoxyl radical and generates the $Fe^{III}HO_2^{2+}$ complex as identified previously. Reaction (61) has an activation energy of 42 kJ/mol [41]. Oxidation of Fe^{2+} by the superoxide radical leads to the formation of Fe(III) and peroxide with a relatively high rate ($k_{62} = 1.0 \times 10^7\ M^{-1}\ s^{-1}$) [26]. The rate constants k_{63} and k_{64} with the complexed forms have been estimated by Santana-Casiano et al. [23] but they result from a global fit and seem somewhat doubtful (k_{62} also determined by this method is abnormally low with $2.0 \times 10^2\ M^{-1}\ s^{-1}$). The value of $1.0 \times 10^7\ M^{-1}\ s^{-1}$ established by Rush and Bielski [26] in the field of pH 1–7 was finally attributed to k_{63} and k_{64} by default. It could be a lower limiting value, considering that rate constants usually increase with the complexation level of Fe^{2+}.

$$Fe^{2+} + HO_2^\cdot \rightarrow Fe^{III}HO_2^{2+} \quad k = 1.2 \times 10^6\ M^{-1}\ s^{-1}\ [41] \tag{61}$$
$$Fe^{2+} + O_2^{\cdot-} \rightarrow Fe^{3+} + O_2^{2-} \quad k = 1.0 \times 10^7\ M^{-1}\ s^{-1}\ [26] \tag{62}$$
$$Fe^{II}OH^+ + O_2^{\cdot-} \rightarrow Fe^{III}OH^{2+} + O_2^{2-}\ k = 1.0 \times 10^7\ M^{-1}\ s^{-1}\ [26] \tag{63}$$
$$Fe^{II}(OH)_2^\circ + O_2^{\cdot-} + H_2O \rightarrow Fe^{III}(OH)_2^+ + O_2^{2-}\ k = 1.0 \times 10^7\ M^{-1}\ s^{-1}\ [26] \tag{64}$$

3.2.4. Reactions of Fe(III) with $HO_2^\cdot$ and $O_2^{\cdot-}$

Ferric iron is reduced by $O_2^{\cdot-} + H_2O/HO_2^\cdot$ radicals to produce ferrous iron and molecular oxygen (Reactions (65)–(68)) with a reactivity which clearly depends on the pH [45]. At a pH below 4.8, the reactivity with $HO_2^\cdot$ is rather weak. Rush and Bielski gave an upper limiting value of $10^3\ M^{-1}\ s^{-1}$ for Reaction (65) which is probably the same for all the Fe(III) species [26]. It is the reason why this limiting value has been also attributed to Reaction (66). Some higher values can be found in the literature [30] for k_{66} but without serious justification. In fact, if the rate constants k_{65} and k_{66} were greater than $10^3\ M^{-1}\ s^{-1}$, then the Fricke dosimeter (based on

Fe^{2+} oxidation into Fe^{3+}) could not be used, becoming non-linear with such "strong" back reactions.

At a pH above 4.8, the attack of the superoxide radical is more efficient in obtaining a Fe(II) complex and dioxygen (Reaction (67)) [26]. Accumulating up to significant concentrations of 10^{-4} M in alkaline solution, the superoxide radical constitutes the dominant reducing species with which the $Fe^{III}(OH)_4^-$ complex reacts probably according to a similar mechanism (Reaction (68)). In the absence of available data, rate constant k_{68} may be considered as being equal at least to k_{67}.

$$Fe^{3+} + HO_2^{\cdot} \rightarrow Fe^{2+} + O_2 + H^+ \quad k \leq 10^3\ M^{-1}\ s^{-1}\ [26] \tag{65}$$

$$Fe^{III}OH^{2+} + HO_2^{\cdot} \rightarrow Fe^{II}OH^+ + O_2 + H^+ \quad k \leq 10^3\ M^{-1}\ s^{-1} \tag{66}$$

$$Fe^{III}OH^{2+} + O_2^{\cdot-} + H_2O \rightarrow Fe^{II}OH^+ + O_2 \quad k = 1.5 \times 10^8\ M^{-1}\ s^{-1}\ [26] \tag{67}$$

$$Fe^{III}(OH)_4^- + O_2^{\cdot-} \rightarrow Fe^{II}(OH)_4^{2-} + O_2 \quad k \geq 1.5 \times 10^8\ M^{-1}\ s^{-1} \tag{68}$$

3.2.5. Reactions of Fe(II) with OH· and O·⁻

The most oxidising radicals of water radiolysis react very quickly with ferrous iron, with radical $O^{\cdot-}$ appearing to be more reactive than its OH· counterpart. Paradoxically, oxidation generates Fe(III), whereas the oxidation induced by peroxides (weaker oxidisers) generates Fe(IV). Reaction (69) has an activation energy of 9 kJ/mol [31]. Since only reactions with Fe^{2+} are available, there is an effective lack of information on the overall alkaline field. With due account of the significance of radicals OH· with regard to the family of reactions, the reactions with $Fe^{II}(OH)_3^-$ were selected with a view to maintaining the consistency of the system. In that framework, the rate constants of Reactions (71) and (72) are identical to those for Reactions (69) and (70), by default, as follows:

$$Fe^{2+} + OH^{\cdot} \rightarrow Fe^{III}OH^{2+} \quad k = 4.5 \times 10^8\ M^{-1}\ s^{-1}\ [31] \tag{69}$$

$$Fe^{2+} + O^{\cdot-} \rightarrow Fe^{3+} + O^{2-} \quad k = 3.8 \times 10^9\ M^{-1}\ s^{-1}\ [46] \tag{70}$$

$$Fe^{II}(OH)_3^- + OH^{\cdot} \rightarrow Fe^{III}(OH)_4^- \quad k = 4.5 \times 10^8\ M^{-1}\ s^{-1} \tag{71}$$

$$Fe^{II}(OH)_3^- + O^{\cdot-} \rightarrow Fe^{III}(OH)_3^{\circ} + O^{2-} \quad k = 3.8 \times 10^9\ M^{-1}\ s^{-1} \tag{72}$$

3.2.6. Reactions of Fe(III) with OH· and O·⁻

Contrary to the previous case, no information is available on the attack by oxidising radicals Fe^{3+} and its slightly-complexed forms. However, in alkaline media (NaOH = 1 M), Rush and Bielski [18] have shown the possibility to form a monomer complex of Fe(IV) from $Fe^{III}(OH)_4^-$ with a high rate constant (bottom limit), which is expressed by the following generic formulations:

$$Fe^{III}(OH)_4^- + OH^{\cdot} \rightarrow Fe^{IV}O(OH)_n^{2-n} + (3-n)OH^- + H_2O \quad k \geq 8.5 \times 10^7\ M^{-1}\ s^{-1}\ [18] \tag{73}$$

$$Fe^{III}(OH)_4^- + O^{\cdot-} \rightarrow Fe^{IV}O(OH)_n^{2-n} + (4-n)OH^- \quad k \geq 8.5 \times 10^7\ M^{-1}\ s^{-1}\ [18] \tag{74}$$

Consistent with the writing of Fe(IV) complexes as above and by taking $n = 2$, Reactions (73) and (74) may be interpreted as follows, maintaining an identical rate constant:

$$Fe^{III}(OH)_4^- + OH^{\cdot} \rightarrow Fe^{IV}(OH)_4^{\circ} + OH^- \tag{75}$$

$$Fe^{III}(OH)_4^- + O^{\cdot-} \rightarrow Fe^{IV}(OH)_4^{\circ} + O^{2-} \tag{76}$$

3.2.7. Reactions of Fe(II) with H· and e_{aq}^-

Although it has been observed at very low pH in the absence of dioxygen, it is worth mentioning the capability of radical H· (normally very reducing) to oxidise Fe(II) into Fe(III) with a significant rate constant (Reaction (77)). That latter reaction has an activation energy of 14 kJ/mol [47]. A homologous reaction with radical e_{aq}^- is also mentioned with a slightly faster rate constant [48]. Reactions (77) and (78) have little impact on the course of the radiolysis in cement media, but may contribute in the capture of a small fraction of the reducing radicals of primary origin in anaerobic environment. The Fe(III) hydride formed in both cases reacts with water (H_3O^+) and produces dihydrogen [49], as follows:

$$Fe^{2+} + H^{\cdot} \rightarrow Fe^{III}H^{2+} \quad k = 5.64 \times 10^7\ M^{-1}\ s^{-1}\ [47] \tag{77}$$

$$Fe^{2+} + e_{aq}^- \rightarrow Fe^{III}H^{2+} + OH^- \quad k = 1.6 \times 10^8\ M^{-1}\ s^{-1}\ [48] \tag{78}$$

$$Fe^{III}H^{2+} + H_3O^+ \rightarrow Fe^{3+} + H_2 + H_2O \quad k = 1.1 \times 10^4\ M^{-1}\ s^{-1}\ [49] \tag{79}$$

3.2.8. Reactions of Fe(III) with H· and e_{aq}^-

Although radicals H· and e_{aq}^- are very powerful as Fe(III) reducers, the two observed reactions with H· help to detect a modulation in the reactivity in relation to pH, with the rate constants increasing with the complexation level of Fe(II) [50,51]. As generally observed, the reaction occurs also faster with the base form of antagonistic species [20]. Described at a pH of 7, Reaction (84) involves the $Fe^{III}(OH)_2^+$ complex with the same rate constant as for Reaction (82) [52]. In the absence of information and in the framework of a possibly generic description (reaction towards undifferentiated Fe(III)), the rate constant of Reaction (83) is considered as identical, as well as Reaction (85), which is added by necessity ($Fe^{III}(OH)_4^-$ prevailing in cement media).

$$Fe^{3+} + H^{\cdot} \rightarrow Fe^{2+} + H^+ \quad k = 7.0 \times 10^5\ M^{-1}\ s^{-1}\ [50] \tag{80}$$

$$Fe^{III}OH^{2+} + H^{\cdot} \rightarrow Fe^{2+} + H_2O \quad k = 1.2 \times 10^9\ M^{-1}\ s^{-1}\ [51] \tag{81}$$

$$Fe^{3+} + e_{aq}^- \rightarrow Fe^{2+} + H_2O \quad k = 6.0 \times 10^{10}\ M^{-1}\ s^{-1}\ [20] \tag{82}$$

$$Fe^{III}OH^{2+} + e_{aq}^- \rightarrow Fe^{II}OH^+ + H_2O \quad k = 6.0 \times 10^{10}\ M^{-1}\ s^{-1}\ \text{(estimate)} \tag{83}$$

$$Fe^{III}(OH)_2^+ + e_{aq}^- \rightarrow Fe^{II}(OH)_2^{\circ} + H_2O \quad k = 6.0 \times 10^{10}\ M^{-1}\ s^{-1}\ [52] \tag{84}$$

$$Fe^{III}(OH)_4^- + e_{aq}^- \rightarrow Fe^{II}(OH)_4^{2-} + H_2O \quad k = 6.0 \times 10^{10}\ M^{-1}\ s^{-1}\ \text{(estimate)} \tag{85}$$

4. Water radiolysis model in the presence of iron

4.1. "Iron" module

Taking into account the reactions including the aqueous species of iron only applies as a complement of the reaction system of water radiolysis. In order to update this latter, which has been the subject of many descriptions in the past [2,53], it is important to address also the case of the H^+ species generated by the reducing reactions of Fe^{3+} with the H· or $HO_2^{\cdot}$ radicals. Based on the formation of the H_3O^+ ion within the solvent (Reaction (86)), the conversion kinetics corresponds to a pseudo-first order by considering $[H_2O] \approx 55.5$ M as constant, as follows:

$$H^+ + H_2O \rightarrow H_3O^+ \qquad \frac{d[H^+]}{dt} = -k[H^+][H_2O] \Rightarrow [H^+]_t = [H^+]_0 \cdot e^{-[H_2O]kt} \tag{86}$$

With a H^+ average lifetime equal to $\tau = 10^{-12}$ s [54], it is possible to deduce the following:

$$[H^+]_\tau = [H^+]_0 \cdot e^{-[H_2O]k\tau} = \frac{[H^+]_0}{e} \quad \text{i.e.}: k_{86} = \frac{1}{\tau[H_2O]} = 1.8 \times 10^{10}\ M^{-1}\ s^{-1}$$

The entire set of elementary reactions having been first collected with the aqueous species of iron is listed in Table 7 according to the following classification: (1) bimolecular reactions, followed by decomposition reactions; (2) reactions first with radicals of water radiolysis, and then with molecular species; and (3) reactions with Fe(II), then with Fe(III), and then with Fe(IV).

Among the 60 or so selected reactions, the collected kinetic data include an uncertainty level that is generally higher than that associated with the "water" system, with more than about 10 estimated rate constants. In addition, only 25% of the reaction data have an activation-energy value. Under such conditions, the simulation results of that system require the utmost caution in their interpretation, especially as we move away from the standard temperature of 25 °C. Among the listed reactions, Fe(IV)-related reactions are the most incomplete and require probably much retouching in the future, particularly regarding the nature of the reactive species and of the products that are actually involved ("oxo" or "hydroxo" forms of Fe(IV)). Although the FeO^{2+} entity probably exists [36], it was decided to convert the "oxo" form of the ferryl ion into the "hydroxo" form (with an arbitrary very high rate constant) in order to be consistent with the different mechanisms that are written also thanks to "hydroxo" species, as follows:

$$FeO^{2+} + H_2O \rightarrow Fe^{IV}(OH)_2^{2+} \quad k = 10^{10}\ M^{-1}\ s^{-1} \tag{87}$$

Note that Reaction (87) is artificial since (1) complexes being hexacoordinate, the addition of water is virtual; (2) it is the reverse reaction which is the most probable according to molecular dynamics simulations [55]:

$$Fe^{IV}(OH)_2(H_2O)_4^{2+} \rightarrow Fe^{IV}O(H_2O)_5^{2+} \tag{88}$$

Complexation equilibria are described successively for the species of Fe(II), Fe(III) and Fe(IV) in Table 8. Each one is presented in the form of dual reactions; the relationship of their rate constants is equal more or less to the equilibrium constant without activity and unit corrections. To the extent that most rate constants are unknown, an arbitrary value is given to the complexation reaction of every equilibrium by increasing each complexation level by an order of magnitude, with the understanding that such rule is taking into account the growing reactivity of the species with the complexation rank. Calculations for the inverse rate constant are illustrated by the following example, where the complexation constant is known:

$$FeOH^{2+} + FeOH^{2+} \rightarrow Fe_2(OH)_2^{4+} \quad k = 4.5 \times 10^2\ M^{-1}\ s^{-1}\ [56] \tag{89}$$

$$Fe_2(OH)_2^{4+} \rightarrow FeOH^{2+} + FeOH^{2+}\ k_R \quad \text{to be determined} \tag{90}$$

At equilibrium, the equality of the reactions kinetics helps in deducing the ratio of the rate constants in terms of noted molar concentrations [Sp], as follows:

$$\frac{k}{k_R} = \frac{[Fe_2(OH)_2^{4+}]}{[FeOH^{2+}]^2}$$

As for the equilibrium constant, it is defined in terms of activities as the product of a γ activity coefficient and a noted molal concentration $[Sp]^*$, as follows:

$$K = \frac{[Fe_2(OH)_2^{4+}]^*\gamma_4}{[FeOH^{2+}]^{*2}\gamma_2^2}$$

In order to integrate only molar concentrations in calculations, molal concentrations are converted according to the following relationship:

$$[Sp]^* = \frac{[Sp]}{CUC} \text{ where } CUC = \frac{10^{-3}\rho_{liq}}{1 + \Sigma_i \mathscr{M}_i[Sp_i]} \times (= 10^{-3}\rho_{H_2O} \text{ with a zero ionic strength})$$

with CUC: coefficient of concentration units conversion $\left(kg_{solvent}/dm^3_{solution}\right)$

ρ_{liq}: density of the solution (kg/m^3),
M_i: molar mass of a species in solution "Sp$_i$" (kg/mol)

With $K = 10^{1.48}$ [57], it becomes ultimately as follows:

$$k_R = \frac{k\gamma_4 CUC}{K\gamma_2^2} = 14.86\ s^{-1} \text{ (with a zero ionic strength)}$$
$$= 1.367\ s^{-1} \text{ (at pH} = 13.223 \text{ and } I = 0.2257)$$

The approach described above is applied to all equilibria, even though the complexation rate constant is unknown. The special case of the $Fe_2(OH)_2^{4+}$ complex may serve to illustrate the fact that the value of rate constants may be influenced significantly by the environment, with the activity of the highly-charged species ($|z| \geqslant 3$) becoming very rapidly quite low with the ionic strength.

With regard to the kinetics of heterogeneous equilibria, this latter shows more specific aspects, with the dissolution rate being a zero order in relation to the solid and the precipitation rate being proportional to the ionic product (in the hypothesis of microreversibility). In the case of the ferrihydrite-solution equilibrium (91), the following formulation applies:

$$Fe(OH)_3 \downarrow \underset{k_{prec}}{\overset{k_{diss}}{\rightleftarrows}} Fe^{3+} + 3OH^- \tag{91}$$

That interpretation implies the following relationship (at equilibrium):

$$\frac{k_{diss}}{k_{prec}} = K_{fer} = [Fe^{3+}][OH^-]^3 \cdot \gamma_3\gamma_1^3 = 10^{-38.1096} \text{ (at 25°C)}$$

In cement media with a pH above 13, however, writing the solubility product based on the constituting ions runs the risk of inducing numerical anomalies in rate calculations, because the concentration of the Fe^{3+} species is extremely low (in the order of 2.5×10^{-35} M, which is equivalent to about 10 molecules per cubic kilometre). In such cases, writing the solubility product on the basis of the dominant species with an alkaline pH is therefore preferable, as follows:

$$Fe(OH)_3 \downarrow \underset{k_{prec}}{\overset{k_{diss}}{\rightleftarrows}} Fe(OH)_4^- - OH^- \tag{92}$$

The new relationship among rate constants and the equilibrium constant, which is independent from activity coefficients after simplification (in this particular case), is modified as follows:

$$\frac{k_{diss}}{k_{prec}} = K'_{fer} = \frac{[Fe(OH)_4^-]}{[OH^-]} = K_{fer} \times K_{FeIII1} \times K_{FeIII2} \times K_{FeIII3} \times K_{FeIII4} = 10^{-2.4797} \text{ (at 25° C)}$$

In the end, the instantaneous variation of ferrihydrite and of the associated aqueous species is described by the relative saturation (the term between parentheses being without dimension), the dissolution rate constant k_{diss} (M s^{-1} m^{-2}) and the mineral surface, S (m^2), as follows:

$$\frac{d[Fe(OH)_3]}{dt} = -k_{diss} \cdot S\left(1 - \frac{[Fe(OH)_4^-]}{[OH^-]K'_{fer}}\right) \text{ (M s}^{-1}\text{)}$$

$$\frac{\partial[Fe(OH)_4^-]}{\partial t} = -\frac{d[Fe(OH)_3]}{dt} \text{ and } \frac{\partial[OH^-]}{\partial t} = \frac{d[Fe(OH)_3]}{dt}$$

Table 7
Reactions and rate constants related to aqueous iron species for radiolysis simulations in cement-based materials; by convention, $e^-_{aq} = H_2O^-$.

No	Reaction	Pre-exponential factor A	Activation Energy EA (kJ/mol)	$k_{25°C}$[a] ($M^1\ s^1$)[b]	Reference
R500	$e^-_{aq} + Fe^{2+} \rightarrow OH^- + FeH^{2+}$			1.6×10^8	[45]
R501	$e^-_{aq} + Fe^{3+} \rightarrow H_2O + Fe^{2+}$			6×10^{10}	[18]
R502	$e^-_{aq} + FeOH^{2+} \rightarrow H_2O + FeOH^+$			6×10^{10}	Estimate
R503	$e^-_{aq} + Fe(OH)^+_2 \rightarrow H_2O + Fe(OH))2^\circ$			6×10^{10}	[49]
R504	$e^-_{aq} + Fek(OH)^-_4 \rightarrow H_2O + Fe(OH)^{2-}_4$			6×10^{10}	Estimate
R505	$H + Fe^{2+} \rightarrow FeH^{2+}$	1.6×10^{10}	14	5.64×10^7	[43]
R506	$H + Fe^{3+} \rightarrow H^+ + Fe^{2+}$			7×10^5	[47]
R507	$H + FeOH^{2+} \rightarrow H_2O + Fe^{2+}$			1.2×10^9	[48]
R508	$O^- + Fe^{2+} \rightarrow O^{2-} + Fe^{3+}$			3.8×10^9	[43]
R509	$O^- + Fe(OH)^-_3 \rightarrow O^{2-} + Fe(OH)^\circ_3$			3.8×10^9	Estimate
R510	$O^- + Fe(OH)^-_4 \rightarrow O^{2-} + Fe(OH)^\circ_4$			8.5×10^7	Estimate
R511	$OH + Fe^{2+} \rightarrow FeOH^{2+}$	1.7×10^{10}	9	4.5×10^8	[29]
R512	$OH + Fe(OH)^-_3 \rightarrow Fe(OH)^-_4$			4.5×10^8	Estimate
R513	$OH + Fe(OH)^-_4 \rightarrow OH^- + Fe(OH)^\circ_4$			8.5×10^7	[16]
R514	$OH + Fe(OH)^{2+}_2 \rightarrow H_2O_2 + FeOH^{2+}$			1×10^7	[12]
R515	$OH + Fe(OH)^+_3 \rightarrow H_2O_2 + Fek(OH)^+_2$			1×10^7	[12]
R516	$OH + Fe(OH)^\circ_4 \rightarrow H_2O_2 + Fe(OH)^\circ_3$			1×10^7	[12]
R517	$O^-_2 + Fe^{2+} \rightarrow O^{2-}_2 + Fe^{3+}$			1.0×10^7	[24]
R518	$O^-_2 + FeOH^+ \rightarrow O^{2-}_2 + FeOH^{2+}$			1×10^7	Estimate
R519	$O^-_2 + Fe(OH)^\circ_2 \rightarrow O^{2-}_2 + Fe(OH)^+_2$			1×10^7	Estimate
R520	$O^-_2 + FeOH^{2+} \rightarrow O_2 + FeOH^+$			1.5×10^8	[24]
R521	$O^-_2 + Fe(OH)^-_4 \rightarrow O_2 + Fe(OH)^{2-}_4$			1.5×10^8	Estimate
R522	$HO_2 + Fe^{2+} \rightarrow FeHO^{2+}_2$	2.737×10^{13}	42	1.2×10^6	[38]
R523	$HO_2 + Fe^{3+} \rightarrow H^+ + O_2 + Fe^{2+}$			1×10^3	[24]
R524	$HO_2 + FeOH^{2+} \rightarrow H^+ + O_2 + FeOH^+$			1×10^3	Estimate
R525	$HO_2 + Fe(OH)^{2+}_2 \rightarrow O_2 + H_2O + FeOH^{2+}$			2×10^6	[12]
R526	$HO_2 + Fe(OH)^+_3 \rightarrow O_2 + H_2O + Fe(OH)^+_2$			2×10^6	[12]
R527	$HO_2 + Fe(OH)^\circ_4 \rightarrow O_2 + H_2O + Fe(OH)^\circ_3$			2×10^6	[12]
R528	$H_2O + FeO^{2+} \rightarrow Fe(OH)^{2+}_2$			1×10^{10}	Estimate
R529	$H_3O^+ + FeH^{2+} \rightarrow H_2O + H_2 + Fe^{3+}$			1.1×10^4	[46]
R530	$H_3O^+ + Fe - H_2O^{2+}_2 \rightarrow 2H_2O + OH + Fe^{3+}$			5.24×10^1	Estimate
R531	$HO^-_2 + Fe^{3+} \rightarrow FeHO^{2+}_2$			9×10^5	[37]
R532	$H_2O_2 + Fe^{2+} \rightarrow Fe - H_2O^{2+}_2$	1.195×10^9	42	5.24×10^1	[36]
R533	$H_2O_2 + FeOH^+ \rightarrow FeOH - H_2O^+_2$	3.206×10^{10}	22.9	3.12×10^6	[25]
R534	$H_2O_2 + Fe(OH)^\circ_2 \rightarrow Fe(OH)_2 - H_2O^\circ_2$	1.95×10^{19}	55.4	3.84×10^9	[25]
R535	$H_2O_2 + Fe^{3+} \rightarrow FeHO^{2+}_2 + H^+$			4.48×10^{-3}	[28]
R536	$H_2O_2 + FeOH^{2+} \rightarrow FeHO^{2+}_2 + H_2O$			2×10^{-2}	[39]
R537	$H_2O_2 + Fe(OH)_22+ \rightarrow HO_2 + H_2O + FeOH^{2+}$	1.017×10^8	23	9.5×10^3	[35]
R538	$H_2O_2 + Fe(OH)^+_2 \rightarrow HO_2 + H_2O + Fe(OH)^+_2$	1.017×10^8	23	9.5×10^3	[35]
R539	$H_2O_2 + Fe(OH)^\circ_4 \rightarrow HO_2 + H_2O + Fe(OH)^\circ_3$	1.017×10^8	23	9.5×10^3	[35]
R540	$O_2 + Fe^{2+} \rightarrow O^-_2 + Fe^{3+}$			8.75×10^{-2}	[21]
R541	$O_2 + FeOH^+ \rightarrow O^-_2 + FeOH^{2+}$			2.41×10^1	[21]
R542	$O_2 + Fe(OH)^\circ_2 \rightarrow O^-_2 + Fe(OH)^+_2$			8.16×10^4	[21]
R543	$O_2 + Fe(OH)^-_3 \rightarrow O^-_2 + Fe(OH)^\circ_3$			1.17×10^9	Estimate
R544	$O_3 + Fe^{2+} \rightarrow O_2 + FeO^{2+}$	5.8×10^{12}	39	8.5×10^5	[35]
R545	$Fe^{2+} + FeHO^{2+}_2 \rightarrow Fe_2HO^{4+}_2$			6.8×10^5	[38]
R546	$Fe^{2+} + Fe(OH)^{2+}_2 \rightarrow Fe^{3+} + Fe(OH)^+_2$	5.995×10^5	7	3.56×10^4	[13]
R547	$Fe^{2+} + Fe(OH)^{2+}_2 \rightarrow Fe_2(OH)^{4+}_2$	1.756×10^{11}	42	7.7×10^3	[13]
R548	$FeOH^+ + Fe(OH)^+_3 \rightarrow 2Fe(OH)^+_2$			1.4×10^5	Estimate
R549	$Fe(OH)^-_3 + Fe(OH)^\circ_4 \rightarrow Fe(OH)^\circ_3 + Fe(OH)^-_4$			1.4×10^5	Estimate
R550	$Fe - H_2O^{2+}_2 \rightarrow H_2O_2 + Fe^{2+}$			1.8×10^{-1}	[26]
R551	$FeOH - H_2O^+_2 \rightarrow H_2O_2 + FeOH^+$			2.18×10^4	[26]
R552	$Fe(OH)_2 - H_2O^\circ_2 \rightarrow H_2O_2 + Fe(OH)^\circ_2$			2.69×10^7	[26]
R553	$Fe - H_2O^{2+}_2 \rightarrow Fe(OH)^{2+}_2$			1.87×10^{-1}	[26]
R554	$FeOH - H_2O^+_2 \rightarrow Fe(OH)^+_3$			1.87×10^{-1}	[26]
R555	$Fe(OH)_2 - H_2O^\circ_2 \rightarrow Fe(OH)^\circ_4$			1.87×10^{-1}	[26]
R556	$Fe_2HO^{4+}_2 \rightarrow FeHO^{2+}_2 + Fe^{2+}$	5.683×10^{12}	47.7	2.5×10^4	[38]
R557	$FeHO^{2+}_2 \rightarrow Fe^{3+} + HO^-_2$	6.614×10^4	8.8	1.9×10^3	[38]
R558	$Fe(OH)^{2+}_2 \rightarrow FeOH^{2+} + OH$	6.529×10^5	34	7.216×10^{-1}	[12]
R559	$Fe(OH)^+_3 \rightarrow Fe(OH)^+_2 + OH$			2	[28]
R560	$Fe(OH)^\circ_4 \rightarrow Fe(OH)^\circ_3 + OH$			2	Estimate

[a] $k = A\exp(-EA/RT)$.
[b] Excepted for R550–R560 (s^{-1}).

Table 8
Acido-basic equilibria and rate constants used for radiolytic chemistry within the cement pore solution with ionic strength I = 0.2257 mol/kg and water activity = 0.9917.

No	Reactions	$k_{25°C}$ (M^{-1} s^{-1})	Reference	Equilibrium	$K(T)$
E570	$Fe^{2+} + OH^- = FeOH^+$	1×10^3	Estimate		$7.7261 \times 10^{-78}\ T^{28.0226}\ e^{8425.31/T}$
E571	$FeOH^+ \rightarrow Fe^{2+} + OH^-$	1.039×10^{-1}		$K_{II/1}$	
E572	$FeOH^+ + OH^- \rightarrow Fe(OH)_2^\circ$	1×10^4	Estimate	$K_{II/2}$	$1.10558 \times 10^{-48}\ T^{18.004}\ e^{4331.73/T}$
E573	$Fe(OH)_2^\circ \rightarrow FeOH^+ + OH^-$	2.265×10^1			
E574	$Fe(OH)_2^\circ + OH^- \rightarrow Fe(OH)_3^-$	1×10^5	Estimate	$K_{II/3}$	$1.16791 \times 10^{-84}\ T^{27.5656}\ e^{12717.5/T}$
E575	$Fe(OH)_3^- \rightarrow Fe(OH)_2^\circ + OH^-$	1.576×10^2			
E576	$Fe(OH)_3^- + OH^- \rightarrow Fe(OH)_4^{2-}$	1×10^6	Estimate	$K_{II/4}$	$2.71533 \times 10^{-7}\ T^{0.0725674}\ e^{4041.73/T}$
E577	$Fe(OH)_4^{2-} \rightarrow Fe(OH)_3^- + OH^-$	1.735×10^6			
E578	$Fe^{3+} + OH^- \rightarrow FeOH^{2+}$	1×10^7	Estimate	$K_{III/1}$	$4.25359 \times 10^{-29}\ T^{13.0728}\ e^{5378.81/T}$
E579	$FeOH^{2+} \rightarrow Fe^{3+} + OH^-$	9.224×10^{-5}			
E580	$FeOH^{2+} + OH^- \rightarrow Fe(OH)_2^+$	1×10^8	Estimate	$K_{III/2}$	$3.2868 \times 10^{-36}\ T^{14.1432}\ e^{7556.64/T}$
E581	$Fe(OH)_2^+ \rightarrow FeOH^{2+} + OH^-$	9.928×10^{-3}			
E582	$Fe(OH)_2^+ + OH^- \rightarrow Fe(OH)_3^\circ$	1×10^9	Estimate	$K_{III/3}$	$6.04496 \times 10^{-7}\ T^{3.16236}\ e^{3780.92/T}$
E583	$Fe(OH)_3^\circ \rightarrow Fe(OH)_2^+ + OH^-$	1.394×10^2			
E584	$Fe(OH)_3^\circ + OH^- \rightarrow Fe(OH)_4^-$	1×10^{10}	Estimate	$K_{III/4}$	$2.97828 \times 10^{-100}\ T^{34.7699}\ e^{13506.7/T}$
E585	$Fe(OH)_4^- \rightarrow Fe(OH)_3^\circ + OH^-$	6.531×10^3			
E586	$FeOH^{2+} + FeOH^{2+} \rightarrow Fe_2(OH)_2^{4+}$	4.5×10^2	[56]	$K_{III/5}$	Unavailable
E587	$Fe_2(OH)_2^{4+} \rightarrow FeOH^{2+} + FeOH^{2+}$	1.367			
E588	$Fe(OH)_2^{2+} + OH^- \rightarrow Fe(OH)_3^+$	1×10^7	Estimate	$K_{IV/1}$	Unavailable
E589	$Fe(OH)_3^+ \rightarrow Fe(OH)_2^{2+} + OH^-$	3.326×10^{-5}			
E590	$Fe(OH)_3^+ + OH^- \rightarrow Fe(OH)_4^\circ$	1×10^8	Estimate	$K_{IV/2}$	Unavailable
E591	$Fe(OH)_4^\circ \rightarrow Fe(OH)_3^+ + OH^-$	2.36×10^{-1}			

Since dissolution surface S is selected arbitrarily, the value of the k_{diss} constant requires generally to be adjusted in order to establish a very fast equilibrium that is slightly competitive with the reaction mechanisms acting in parallel. On the basis of the selected definition for the solubility of ferrihydrite, a value for k_{diss} in the order of 10^{-5} M^{-1} s^{-1} m^{-2} helps in attaining a stable equilibrium over time.

4.2. Simulation of Fe(II) self-oxidation

The example of Fe(II) self-oxidation due to atmospheric dioxygen is interesting because, all by itself, it calls upon most of the mechanisms of the "iron module", without any intervention of a radiation source and, consequently, without radiolysis (see Section 3.1.3). Under such conditions, the (virtual) case of a cement pore liquid that was initially at equilibrium with air ($[O_2] = 2.6 \times 10^{-4}$ M) and containing ferrous iron at a fictitious concentration 10^{-4} M constitutes a useful test to assess the behaviour of the chemical system developed previously. Considering a temperature of 25 °C, a closed medium and a pH of 13.23, the evolution of the system should normally induce the fast oxidation of the initial stock of ferrous iron.

By simulating the process over a 1-h period, it is possible to observe effectively the very fast conversion of Fe(II) into Fe(III), accompanied by the momentary appearance of Fe(IV) (Fig. 6a). During the process, for which the precipitation of the hydroxide of ferrous or ferric iron is deliberately neglected, the kinetics relating to the disappearance of Fe(II) and Fe(IV) is similar, since the behaviour of both oxidation states is strongly correlated by the Fe(II) + Fe(IV) → 2 Fe(III) symproportionation reaction. By representing the evolution of the system with a logarithmic scale, it is possible to observe more in detail very short transient steps and to follow in parallel the different oxygen species involved in the process. Fig. 6b shows more particularly:

- the early appearance of Fe(IV) in relation to Fe(III) before the deadline of 1 μs;
- the identical production of Fe(III) and of the superoxide radical up to 0.1 s with a plateau corresponding to the initial concentration of Fe(II);
- the correlated evolution of the superoxide radical, of Fe(II) and of Fe(IV) after 10^{-4} s, with the preservation of a stationary concentration up to 0.1 s, followed by a fast disappearance;
- the modest, but fast, appearance of peroxide up to 10^{-4} s, the time from which the concentration of all species stabilises temporarily; a second production phase, which counterbalances the decline of the superoxide radical, helps in reaching a concentration equal to 50% of the initial Fe(II); and
- the maximum consumption of aqueous O_2 shortly after 10^{-4} s, followed by a slight increase after 0.1 s, which is associated with the disappearance of the superoxide radical.

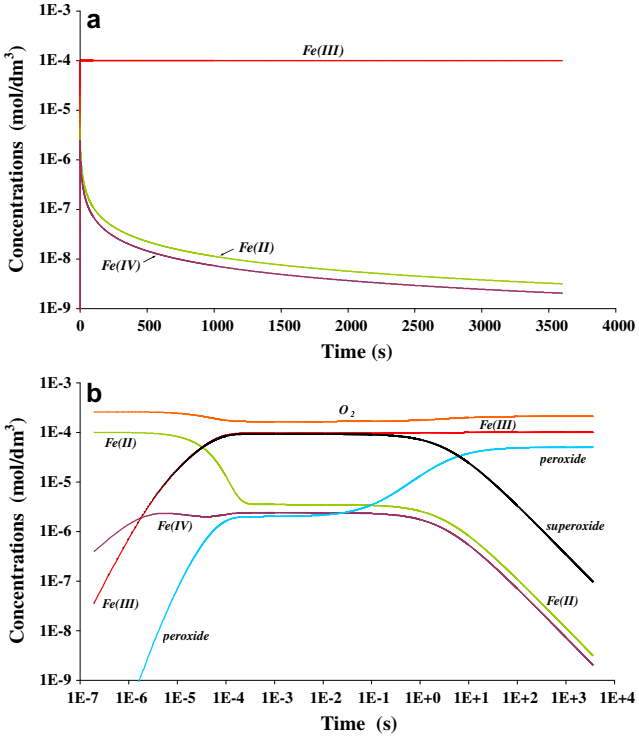

Fig. 6. Simulation of Fe(II) self-oxidation in a confined and initially-aerated neat cement paste, (a) with natural time scale and (b) with logarithmic time scale.

In brief, the self-oxidation of ferrous iron occurs in two successive phases separated by an interval during which all species co-exist with plateau concentrations. By comparing the initial and final calculated concentrations over a 1-h simulation, the following assessment may be drawn:

$$\begin{matrix}[Fe(II)] = 10^{-4}\\ M[O_2] = 2.6\times10^{-4}\,M\end{matrix} \Rightarrow \begin{matrix}[Fe(III)] = 10^{-4}\,M\\ [O_2] = 2.1\times10^{-4}\,M\\ [H_2O_2] = 0.5\times10^{-4}\,M\end{matrix} \Rightarrow [O_2]_\infty = 2.35\times10^{-4}\,M$$

Knowing that 1 mol of metastable H_2O_2 generates 0.5 mol of O_2, the overall dioxygen consumption for the full oxidation of ferrous iron is equal to 0. 25×10^{-4} M (i.e., 1 mol of O_2 for 4 Fe(II)). That balance is therefore consistent with the following overall theoretical redox scheme:

$$4Fe(II) + O_2 \rightarrow 4Fe(III) + 2O^{2-} \quad (93)$$

In conclusion, the implementation of the full kinetic model (water module + iron module) in the framework of the test case for the self-oxidation of Fe(II) was not marred by special behaviour anomalies (excessive accumulation of transient species, drift of pH and of the ionic force, etc.). The iron module may therefore be used to simulate radiolysis in cement media in the framework of a preliminary investigation.

4.3. Radiolysis simulation in cement media

In the perspective of confirming the increase in the production of H_2 in the presence of iron, a provisional test simulation was performed. In order to demonstrate the role of iron without ambiguity, the simulated experiment calls for the gamma irradiation (^{60}Co) of two batches of pure cement pastes, one as a control and the other to which was added ferrihydrite ($Fe(OH)_3$) in excess. The simplified cement pore liquid is considered as a 0.24 mol/kg NaOH solution saturated with portlandite (in reference to the hydration of the previously investigated Portland cement [2]) and ferrihydrite (optional). With the intention of inducing a significant radiolysis of the pore liquid within the materials, a dose rate equal to 0.3 Gy/s was applied (i.e., approximately 1 kGy/h). Due to the inevitable energy deposition associated with such a dose rate, the resulting heat requires that the test be conducted at a temperature of 45 °C. Cement materials are irradiated in sealed 500-cm^3 cylindrical mini-containers with a gas blanket of 290 cm^3. Total porosity of the cement materials is $n = 0.22$ and is occupied at 80% by the liquid phase. Irradiation lasts for 12 months in order to implement a stationary regime within the physico-chemical system. Taking into account a medium that was initially aerated and heated to a temperature of 45 °C, the pore liquid ends up with the detailed composition shown in Table 9. In accordance with the variation of the ferrihydrite solubility with the temperature (see Section 2.2.3), the total concentration of iron in solution increases slightly by 7.4% in relation to that calculated at 25 °C. Based on the descriptive elements given above and the physico-chemical model (radiation chemistry and gas transport), the simulated radiolysis is carried out with the *CHEMSIMUL* software [58].

Table 9
Composition (molar) calculated at 45 °C of a simplified OPC pore solution resulting of equilibrium with portlandite and ferrihydrite.

Cations	Molecules	Anions
$[H_3O^+] = 3.181\times10^{-13}$	$[Ca(OH)_2^\circ] = 2.145\times10^{-4}$	$[OH^-] = 2.218\times10^{-1}$
$[Ca^{2+}] = 4.645\times10^{-4}$	$[NaOH^\circ] = 1.697\times10^{-2}$	$[Fe(OH)_4^-] = 7.968\times10^{-4}$
$[CaOH^+] = 8.010\times10^{-4}$	$[H_2O] = 55.0007$	
$[Na^+] = 2.208\times10^{-1}$	$[H_2] = 3.307\times10^{-10}$	
$[Fe^{3+}] = 2.611\times10^{-34}$	$[O_2] = 1.865\times10^{-4}$	
$[FeOH^{2+}] = 4.436\times10^{-24}$	$[N_2] = 3.759\times10^{-4}$	
$[Fe(OH)_2^+] = 4.854\times10^{-15}$	$[Fe(OH)_3^\circ] = 4.205\times10^{-9}$	
$[Fe_2(OH)_2^{4+}] = 3.578\times10^{-45}$		

Qualitatively speaking, the evolution of the gas phase within the dead volume of the containers is consistent with the radiolysis results of aerated alkaline water (with or without iron) generating simultaneously H_2 and O_2 (Fig. 7). By comparing simulations conducted with and without $Fe(OH)_3$, it is possible to observe a higher net production of H_2 in the presence of iron (Fig. 8a), thus confirming the hypothesis of the mechanism described in the introduction, in other words, the disturbance of the Allen's chain reaction by Fe(II) and Fe(III) species. In the presence of iron, the production of O_2 is also privileged, although the observed excess is twice lower than H_2. Overall, the increase of the partial pressures of H_2 and O_2 in the presence of iron has a progressive impact on the total pressure over time. After 1 year, the increase is significant, being in the order of 60% in comparison with the radiolysis in the absence of ferrihydrite. In a closed system, the recycling rate of H_2 during radiolysis is highly reduced in the presence of ferrihydrite (Fig. 8b), which means that the effective calculated production is close to the primary theoretical production. It should be remembered that the recycling rate is equal to the following:

$$R = 1 - \frac{\left(\frac{d\Sigma[H_2]}{dt}\right)_{\text{effective}}}{\left(\frac{d[H_2]}{dt}\right)_{\text{primary}}}$$

$$\text{where}\left(\frac{d[H_2]}{dt}\right)_{\text{primary}} = \frac{10^{-3}\rho_{liq} - \Sigma\mathscr{M}_i[C_i]}{c_{en}\mathscr{N}_A}\times G(H_2)\times D'$$

$$\text{and}\ \left(\frac{d\Sigma[H_2]}{dt}\right)_{\text{effective}} = \left(\frac{d[H_2]}{dt}\right)_{\text{effective}} + \left(\frac{d[H_2g]}{dt}\right)_{\text{effective}}$$

with $G(H_2)$ being the primary output of H_2 (molecule/heV); D', the dose rate (Gy/s); ρ_{liq}, the density of the pore solution (kg/m^3); $\mathscr{M}_i$, the molar mass of the solute i (kg/mol); $[C_i]$, the molar concentration of the solute i (M); c_{en}, the energy-conversion coefficient (1.60218×10^{-17} J/heV); N_A, the Avogadro constant (6.02214199×10^{23} molecules/mol); $[H_2]$, the molar concentration of H_2 in solution (M), and $[H_2g]$, the quantity of H_2 in the gas phase as referred to the solution volume (mol/dm^3).

In the presence of iron, the significant reduction of the recycling rate by a factor of approximately 2 reflects quantitatively the efficiency loss of the Allen's chain reaction to eliminate H_2 and H_2O_2.

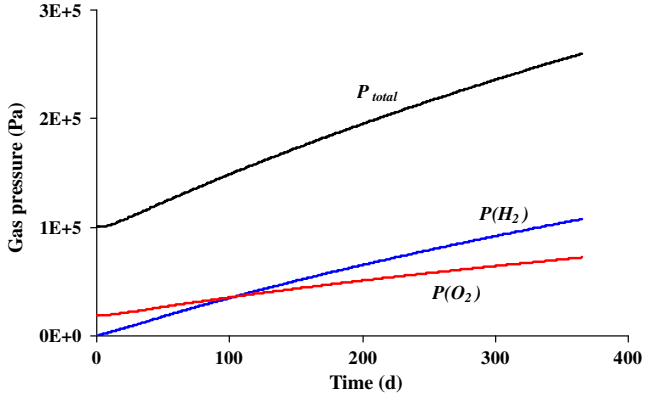

Fig. 7. Evolution of gas pressures (simulation) in the gas blanket with a confined and initially-aerated cement matrix under gamma radiation at 0.3 Gy/s and 45 °C (N_2 and H_2O vapour are not plotted) in the presence of $Fe(OH)_3$.

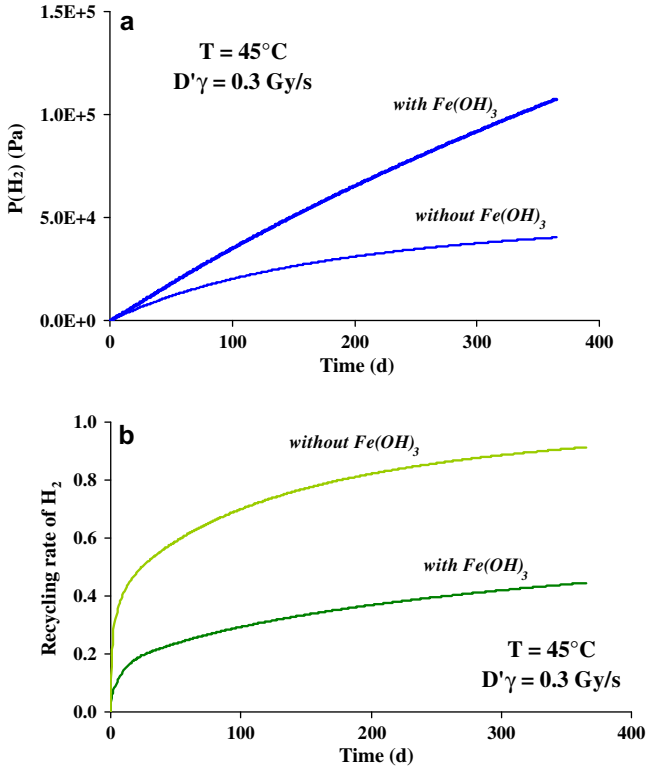

Fig. 8. Radiolysis simulation in a confined and initially-aerated cement matrix in relation to the presence of $Fe(OH)_3$. (a) Comparison of radiolytic H_2 production with calculated pressures in the gas blanket (V_{bl} = 289 cm^3) and (b) comparison of the corresponding H_2 recycling rates.

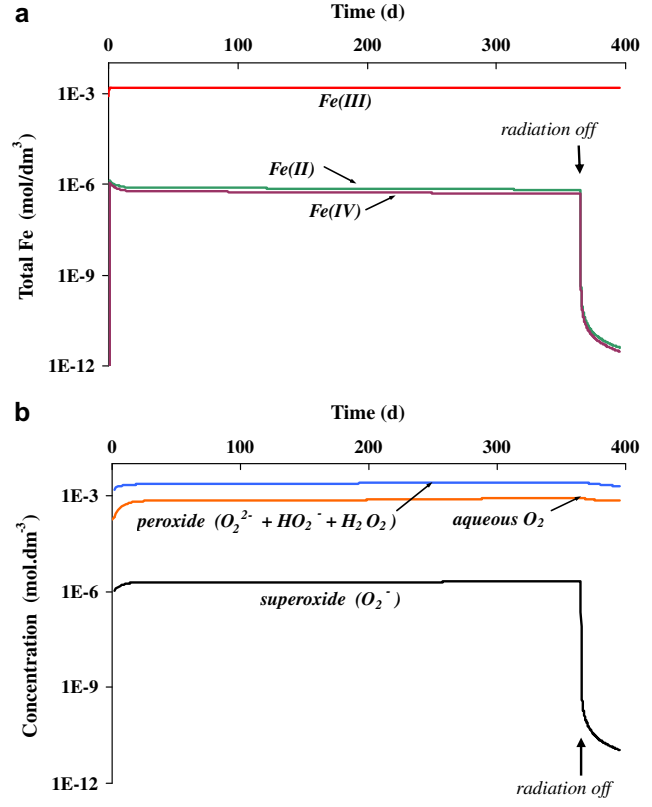

Fig. 9. Radiolysis simulation in a confined and initially-aerated cement medium in the presence of $Fe(OH)_3$. (a) Iron concentration shown for every oxidation level and (b) concentration of the reactive species of oxygen.

Besides the follow-up of the species involved in water radiolysis, the simulation provides also the follow-up of the speciation of iron under irradiation (Fig. 9a). The major informations include the following:

- starting only from Fe(III), radiolysis leads very rapidly to the simultaneous appearance of Fe(II) and Fe(IV); the concentration of which are very close;
- throughout radiolysis, Fe(II), Fe(III) and Fe(IV) co-exist;
- after a transient period of about 20 days, the irradiation maintains a stationary regime with regard to the respective concentrations of Fe(II) and Fe(IV) (high correlation), with Fe(III) being constant by definition, because it is controlled by a mineralogical equilibrium;
- the concentrations of Fe(II) and Fe(IV) are approximately 2500 times lower than those of Fe(III); although they decrease very slowly in parallel with the radioactive decay of the ^{60}Co source, because they are associated with the production of radicals, they are far from being negligible with a few tenths of micromoles per cubic decimetre.

As observed in the description of elementary mechanisms, the presence of iron in solution has a strong impact on the concentration of the reactive oxygen species (ROS). The follow-up of the three oxidation levels of oxygen during radiolysis (0: molecular oxygen, −½: superoxide, −1: peroxide) shows a very high concentration of peroxide exceeding 10^{-3} M and a three times smaller concentration of molecular oxygen (Fig. 9b). That result is the direct consequence of the inhibition of the Allen's chain reaction within which H_2O_2 is involved to the same extent as H_2. From another point of view, Fig. 9a and b show that when irradiation is over, Fe(II), Fe(IV) and $O_2^{\cdot-}$ radical disappear with approximately the same behaviour, which indicates a high correlation between these species. The fact that, in the presence of ferric iron in solution, the cement medium under irradiation hosts high concentrations of oxidising species may eventually modify the understanding of corrosion mechanisms within closed systems (to be relativised however with the mineralogical source of iron). That need for better knowledge was felt recently during the interpretation of corrosion experiments under irradiation showing a kinetic acceleration [59].

From the standpoint of radiolytic chemistry in calcium media, the very high concentration level of peroxide raises an issue in the description of the system's long-term evolution, since such a concentration should normally induce the precipitation of calcium peroxide ($CaO_2{\cdot}8H_2O$) [2]. If that precipitation were to occur, it could generate very rapidly a regulation of the peroxide concentration in the pore solution and, consequently, a regulation of the overall chemical system (O_2, H_2, etc.). In the present case, the

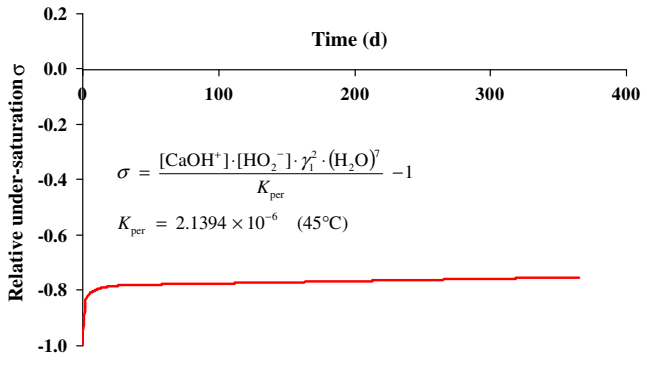

Fig. 10. Radiolysis simulation in a confined initially aerated medium, in the presence of $Fe(OH)_3$, with the evolution of the relative under-saturation in relation to $CaO_2{\cdot}8H_2O$.

temperature of 45 °C favours the dissolution of $CaO_2{\cdot}8H_2O$, and the solubility product of that phase is never reached during radiolysis (Fig. 10), thus creating a relatively monotonous evolution of the chemical system. On the other hand, it is likely that, at 25 °C, precipitation would occur and generate a more complex evolution of the system (with modified production kinetics for H_2 and O_2).

5. Conclusion

During the gamma irradiation of cement-based materials, the presence of iron is an objective cause for the disturbance of the Allen's chain reaction in the water radiolysis scheme. The interaction of radicals e^-_{aq} and $OH^{\cdot}$ with Fe^{3+} and Fe^{2+}, respectively, thus generates a dynamic redox equilibrium, the establishment of which is faster than that corresponding to the Allen's mechanism. Consequently, a large part of the radiolytic products H_2O_2 and H_2 are preserved within a closed system.

In the perspective of completing the radiolytic model in a cement medium with species of iron in solution, the basic data relating to the complexation equilibria of Fe(II) and Fe(III) were gathered together. On the basis of the selected basic species, the list of reactions with the radicalar and molecular products of radiolysis highlights about 60 mechanisms (according to current knowledge). In cement media where $Fe^{III}(OH)_4^-$ constitutes more than 99.9% of the iron in solution, this latter can reach oxidation levels II and IV under gamma irradiation, essentially by reaction with radicals e^-_{aq} and $OH^{\cdot}$. The interaction of Fe(II) with peroxide ("Fenton's reaction") does not constitute an elementary mechanism: with the reversible formation of a transient complex involving Fe(II)–H_2O_2, it seems acknowledged henceforth that radical $OH^{\cdot}$ is the main product only at very low pH while ferryl-based complexes ($Fe^{IV}(OH)_2^{2+}$ to $Fe^{IV}(OH)_4^{\circ}$) become the main oxidising species being formed at higher pH.

Simulation of the self-oxidation of Fe(II) by dioxygen (separate example from the use of a radiation source) with the newly-introduced iron module shows the fast conversion of the initial inventory of Fe(II) into Fe(III) with the transient appearance of Fe(IV), superoxide radicals and of peroxide. The evolution of the different oxidation states of iron seems indissociable from that of the reactive species of oxygen (ROS). Following that preliminary test, an exploratory simulation of the water radiolysis within a cement medium was made at 45 °C in equilibrium with ferrihydrite. As expected, a larger production of radiolytic H_2 is obtained in the presence of iron. Valences II and IV of iron reach a stationary concentration above 0.1 μM, in relation with the constant primary production of radicals, while peroxide and dioxygen present a significant concentration level of ($\approx 10^{-3}$ M after 1 year).

As a general conclusion, the "iron" module combined with the standard model for water radiolysis in cement media proves to be operational for conducting application calculations on an exploration basis. Nevertheless, the preliminary version as presented requires many complements and readjustments before providing a more affirmed predictive character. In that perspective, the chemical system of iron must be developed with the introduction of at least new complexes for Fe(II) and Fe(III) (e.g., sulphate) and new reaction data. Moreover, the model should help corrosion specialists in enhancing the interpretation of occurring phenomena under irradiation, and ultimately, in addressing radiolysis-corrosion couplings.

Acknowledgement

The author thanks gratefully Erling Blergbakke for his advice and for his helpful suggestions, especially concerning the data consistency with regard to acidic media.

References

[1] A.O. Allen, C.J. Hochanadel, J.A. Ghormley, T.W. Davis, J. Phys. Chem. 56 (1952) 575–586.
[2] P. Bouniol, E. Bjergbakke, J. Nucl. Mater. 372 (2008) 1–15.
[3] N.E. Bibler, E.G. Orebaugh, Report DP-1459, Savannah River Laboratory, 1977.
[4] N.E. Bibler, Report DP-1464, Savannah River Laboratory, 1978.
[5] P. Rotureau, J.P. Renault, B. Lebeau, J. Patarin, J.C. Mialocq, ChemPhysChem 6 (2005) 1316–1323.
[6] S. Le Caër, P. Rotureau, F. Brunet, T. Charpentier, G. Blain, J.P. Renault, J.C. Mialocq, ChemPhysChem 6 (2005) 2585–2596.
[7] P. Bouniol, Bétons spéciaux de protection, in Traité de génie nucléaire, Techniques de l'ingénieur, BN3740, 2001, pp. 1–29.
[8] B. Lothenbach, T. Matschei, G. Möschner, F.P. Glasser, Cem. Concr. Res. 38 (2008) 1–18.
[9] B. Lothenbach, E. Wieland, Waste Manage. 26 (2006) 706–719.
[10] J. Chivot, Thermodynamique des produits de corrosion, Rapport ISBN 2-9510108-6-9, Andra, 2004.
[11] M.W.J. Chase, NIST-JANAF thermochemical tables, J. Phys. Chem. Ref. Data Monogr. 9 (1998) 1–1951.
[12] F. Jacobsen, J. Holcman, K. Sehested, Int. J. Chem. Kinet. 30 (1998) 215–221.
[13] S.J. Hug, O. Leupin, Environ. Sci. Technol. 37 (2003) 2734–2742.
[14] T. Løgager, J. Holcman, K. Sehested, T. Pedersen, Inorg. Chem. 31 (1992) 3523–3529.
[15] O. Pestovsky, A. Bakac, J. Am. Chem. Soc. 126 (2004) 13757–13764.
[16] F. Haber, J.J. Weiss, Proc. Roy. Soc. Lond. A (1934) 147–332.
[17] W.C. Bray, M.H. Gorin, J. Am. Chem. Soc. 54 (1932) 2124–2125.
[18] J.D. Rush, B.H.J. Bielski, J. Am. Chem. Soc. 108 (1986) 523–525.
[19] J.D. Rush, Z. Zhao, B.H.J. Bielski, Free Rad. Res. 24 (1996) 187–198.
[20] C.D. Jonah, J.R. Miller, M.S. Matheson, J. Phys. Chem. 81 (1977) 1618–1622.
[21] G.V. Buxton, C.L. Greenstock, W.P. Helman, A.B. Ross, J. Phys. Chem. Ref. Data 17 (1988) 513–886.
[22] F.J. Millero, M. Izaguirre, J. Solution Chem. 18 (1989) 585–599.
[23] J.M. Santana-Casiano, M. Gonzalez-Davila, F.J. Millero, Environ. Sci. Technol. 39 (2005) 2073–2079.
[24] D.W. King, Environ. Sci. Technol. 32 (1998) 2997–3003.
[25] K.M. Rosso, J.J. Morgan, Geochim. Cosmochim. Acta 24 (2002) 4223–4233.
[26] J.D. Rush, B.H.J. Bielski, J. Phys. Chem. Res. 89 (1985) 5062–5066.
[27] M. Gonzalez-Davila, J.M. Santana-Casiano, F.J. Millero, Geochim. Cosmochim. Acta 69 (2005) 83–93.
[28] G. Tachiev, J.A. Roth, A.R. Bowers, Int. J. Chem. Kinet. 32 (2000) 24–35.
[29] J. Weinstein, B.H.J. Bielski, J. Am. Chem. Soc. 101 (1979) 58–62.
[30] S.H. Bossmann, E. Oliveros, S. Göb, S. Siegwart, E.P. Dahlen, L. Payawan, M. Straub, M. Wörner, A.M. Braun, J. Phys. Chem. A 102 (1998) 5542–5550.
[31] H. Christensen, K. Sehested, Radiat. Phys. Chem. 18 (1981) 723–731.
[32] W.H. Koppenol, Redox Rep. 6 (2001) 229–234.
[33] E. Bjergbakke, K. Sehested, O.L. Rasmussen, H. Christensen, Report RIS∅ M-2430, Risø National Laboratory, 1984.
[34] J.J. Pignatello, E. Oliveros, A. MacKay, Crit. Rev. Environ. Sci. Technol. 36 (2006) 1–84.
[35] M.L. Kremer, J. Phys. Chem. A 107 (2003) 1734–1741.
[36] O. Pestovsky, A. Bakac, Inorg. Chem. 45 (2006) 814–820.
[37] F. Jacobsen, J. Holcman, K. Sehested, Int. J. Chem. Kinet. 29 (1997) 17–24.
[38] S. Rachmilovich-Calis, A. Masarwa, N. Meyerstein, D. Meyerstein, R. van Eldik, Chem. Eur. J. 15 (2009) 8303–8309.
[39] H. Christensen, K. Sehested, T. Løgager, Radiat. Phys. Chem. 41 (1993) 575–578.
[40] Y.N. Kozlov, A.D. Nadezhdin, A.P. Pourmal, Int. J. Chem. Kinet. 6 (1974) 383–394.
[41] G.G. Jayson, B.J. Parsons, A.J. Swallow, J. Chem. Soc. Faraday Trans. 69 (1973) 236–242.
[42] C. Walling, A. Goosen, J. Am. Chem. Soc. 95 (1973) 2987–2991.
[43] H. Gallard, J. de Laat, B. Legube, New J. Chem. (1998) 263–268.
[44] J. de Laat, T. Giang Le, Environ. Sci. Technol. 39 (2005) 1811–1818.
[45] K. Sehested, E. Bjergbakke, O.L. Rasmussen, H. Fricke, J. Chem. Phys. 51 (1969) 3159–3166.
[46] D. Zehavi, J. Rabani, J. Chem. Phys. 75 (1971) 1738–1744.
[47] F.S. Dainton, B.J. Holt, N.A. Philipson, M.J. Pilling, J. Chem. Soc. Faraday Trans. 72 (1976) 257–267.
[48] J.H. Baxendale, E.M. Fielden, J.P. Keene, Proc. Roy. Soc. Lond. A 286 (1965) 320–336.
[49] G.G. Jayson, J.P. Keene, D.A. Stirling, A.J. Swallow, Trans. Faraday Soc. 65 (1969) 2453–2464.
[50] G. Navon, G. Stein, J. Phys. Chem. 70 (1966) 3630–3640.
[51] J.H. Baxendale, R.S. Dixon, D.A. Stott, Trans. Faraday Soc. 64 (1968) 2398–2401.
[52] C.L. Greenstock, C. Banerjee, G.W. Ruddock, Proc. Fourth Tihany Symposium on Radiation Chemistry (Keszthely, Hungary, 1–6 June 1976), in: P. Hedvig, R. Schiller (Eds.), Akad. Kiado, Budapest, 1977, pp. 871–879.
[53] P. Bouniol, État des connaissances sur la radiolyse de l'eau dans les colis de déchets cimentés et son approche par simulation, Rapport CEA-R-6069, Direction des systèmes d'information CEA/Saclay, 2004.

[54] G.V. Lagodzinskaya, N.G. Yunda, G.B. Manelis, Chem. Phys. 282 (2002) 51–61.
[55] B. Ensing, F. Buda, P.E. Blöchl, E.J. Baerends, Phys. Chem. Chem. Phys. 4 (2002) 3619–3627.
[56] H. Wendt, Inorg. Chem. 8 (1969) 1527–1528.
[57] A.E. Martell, R.M. Smith, Critical stability constants, Other Organic Ligands, vol. 3, Plenum Press, New York, 1977.
[58] P. Kirkegaard, E. Bjergbakke, J.V. Olsen, CHEMSIMUL: A Chemical Kinetics Software Package, Report Risø-R-1630(EN), Risø DTU dec., 2008.
[59] N.R. Smart, A.P. Rance, L.O. Werme, J. Nucl. Mater. 379 (2008) 97–104.